# HYDRIDE GENERATION AND LASER SPECTROSCOPY TECHNIQUES FOR TRACE ANALYTICAL MEASUREMENTS OF ANTIMONY AND SELENIUM

By

Sangeetha Chari

Submitted in Partial fulfillment of the Requirements

for the degree of

Masters of Science

in the

Chemistry

Program

**YOUNGSTOWN STATE UNIVERSITY**

**AUGUST 2008**

**HYDRIDE GENERATION AND LASER SPECTROSCOPY TECHNIQUES FOR TRACE ANALYTICAL MEASUREMENTS OF ANTIMONY AND SELENIUM**

Sangeetha Chari

I hereby release this thesis to the public. I understand that this thesis will be made available from the OhioLINK ETD Center and the Maag Library Circulation Desk for public access. I also authorize the University or other individuals to make copies of this thesis as needed for scholarly research.

Signature:

_____

Sangeetha Chari Date

Approvals:

_____

Dr. Josef B. Simeonsson Date
Thesis Advisor

_____

Dr. Daryl W. Mincey Date
Committee Member

_____

Dr. Timothy R. Wagner Date
Committee Member

_____

Peter J. Kasvinsky Date
Dean of School of Graduate Studies & Research

## ABSTRACT

Hydride generation (HG) sample introduction increases the sensitivity for certain metal species by converting them to their gaseous forms for measurement by atomic spectrometry techniques. In this work, measurement methods have been developed for the trace analysis of antimony (Sb) and selenium (Se) using HG coupled to Laser Induced Fluorescence (LIF) or Laser Induced Breakdown Spectroscopy (LIBS) detection techniques. In the LIF studies, aqueous samples of Sb are subjected to HG and the Sb hydride is carried to the flame which acts as an atomization source. The wavelengths of absorption and fluorescence emission for Sb were found to be 212.7 nm and 259.8 nm, respectively. The intensity of fluorescence was plotted against the concentration of Sb used. It was found that the intensity was linearly related to the concentration of Sb in the range 0.3-10 ppb. The limit of detection (LOD) was found to be 0.003 ppb. A similar technique has been used for the determination of Sb and Se in aqueous samples using LIBS. In this approach, a plasma instead of a flame is used to excite Sb and Se atoms and the atomic emission is measured at wavelengths of 259.9 nm and 196.1 nm, respectively. Using these wavelengths, calibration curves were plotted for intensity of emission against different concentrations of Sb and Se. From the calibration curve, the slope and LOD have been determined. The results of the studies have been evaluated to show the relative performance of each technique.

## ACKNOWLEDGMENTS

First and foremost I offer my sincere gratitude to my research advisor Dr. Josef B. Simeonsson who has supported me throughout my academics, research work and thesis with his patience and knowledge whilst allowing me the room to work in my own way. I attribute the level of my Masters degree to his encouragement and effort and without him this thesis, too, would not have been completed or written.

I would like to thank all my friends at Youngstown State University and my research group members for their support throughout my academic career. I express my immense appreciation to my committee members, Dr. Timothy R. Wagner and Dr. Daryl W. Mincey for their support and guidance. I would also like to take this opportunity to thank the Department of Chemistry and Graduate School, Youngstown State University for funding me to pursue my masters.

I cannot end without thanking my family, on whose constant encouragement and love I have relied throughout my time at the Academy. I am also grateful to my friend for life, Bharathi whose unflinching courage and conviction has always inspired me to achieve higher in life. It is to them that I dedicate this work.

## TABLE OF CONTENTS

## LIST OF FIGURES

## LIST OF TABLES

## LIST OF SYMBOLS AND ABBREVIATIONS

US-EPA……United States Environmental Protection Agency

LASER……..…… Light Amplification by Stimulated Emission of Radiation

Nd:YAG……..……...Neodymium-doped yttrium aluminum garnet

KDP…….. Potassium dihydrogen phosphate

KD*P……... Potassium dideuterium phosphate

PDA……... Photodiode array

CCD……...Charge coupled device

CID.....Charge injection device

RSS……..Repetitive Single Spark

ND……Neutral Density

DCP……Direct-Current Plasma

MCP……..Microwave-induced Plasma

GLS……..Gas Liquid Separator

AAS……..Atomic Absorption Spectroscopy

AFS……Atomic Fluorescence Spectroscopy

AES……..Atomic Emission Spectroscopy

HG……..……Hydride generation

LIF…….……Laser Induced Fluorescence

LIBS.……..……..Laser Induced Breakdown Spectroscopy

ICP-AES……Inductively Coupled Plasma Atomic Emission Spectroscopy

FAAS……Flame atomic absorption spectrometry

GC……Gas Chromatography

MS……...Mass Spectrometry

ICP-MS……...Inductively coupled plasma Mass spectrometry

HPLC…….. High performance liquid chromatography

HG-AAS……. Hydride generation atomic absorption spectrometry

HG-AFS…….. Hydride generation atomic fluorescence spectrometry

PMT……..……Photomultiplier tube

RF……..…..……Radiofrequency

Sb……...Antimony

Se……Selenium

Al…….Aluminium

Fe……Iron

Mn……Manganese

Sn……..……...Tin

As……...Arsenic

Te……...Tellurium

A……..Absorbance

Ar…….……Argon

$H_2$……...Hydrogen

He…….……..Helium

ppm…….…….Parts per million

ppb……..…….Parts per billion

ppt……..…….Parts per trillion

LOD…….……Limit of detection

LOQ……..……Limit of quantification

RSD……Relative standard deviation

HCl……Hydrochloric acid

$NaBH_4$……..…….……..…..……Sodium Borohydride

NaOH……..…….Sodium hydroxide

NaCl……Sodium Chloride

TRIS……Hydroxymethyl amino methane

L…….……Liter

mL……milliliter

kg……...Killogram

µg…….Microgram

ng……...Nanogram

r.p.m……...revolutions per minute

mm……..…..Millimeter

nm…….Nanometer

µs……...……Microsecond

ns…….…...Nanosecond

µm……...Micrometer

M……..…...Molar

m/v……..……..mass per volume

v/v……..volume per volume

V……..……Volts

mV…….……Millivolts

eV……..……Electronvolt

kW……Kilowatt

µJ…….……...Microjoules

mrad…….……Milliradian

Hz…….……Hertz

MHz……Mega Hertz

K……..……Kelvin

$^{o}$C……...Degree Celsius

% …….....percentage

a.u……..……arbitrary units

$t_d$……..Time Delay

$t_w$……Time Width

σ……..Standard Deviation

sccm……..Standard cubic centimeters per minute

psi……..Pounds per square inch

# CHAPTER 1: INTRODUCTION

## 1.1. BACKGROUND:

### 1.1.1. ATOMIC SPECTROSCOPY:

The main aim of analytical atomic spectroscopy is to identify elements and quantify them in various media. Atomic emission spectroscopy involves atom formation, excitation and emission. For an excitation to occur, the element of interest should be separated from its sample matrix so that its atomic emission spectra are free from interferences. The energy of excitation should be sufficiently high to raise the electron from the ground state to the excited state. After the electron reaches the excited state, the atom emits light, which is characteristic of that particular element.[1]

### 1.1.2. ORIGIN OF SPECTRA:

In an atom, the outer electrons are found in orbitals with well-defined energy levels. When an atom remains unexcited, all of its electrons are in the lowest permitted energy levels. Higher orbitals are empty and represent vacant permitted energy levels. If an atom is excited, its electrons are able to move from a low-energy orbital to an orbital with higher energy or an excited state. The excited atom is then able to emit a photon of energy and its electron returns to a lower-energy state. The emitted radiation from excited atoms is the basis of emission spectroscopy.[2]

The origin of the spectra is shown in Figure 1.[1]

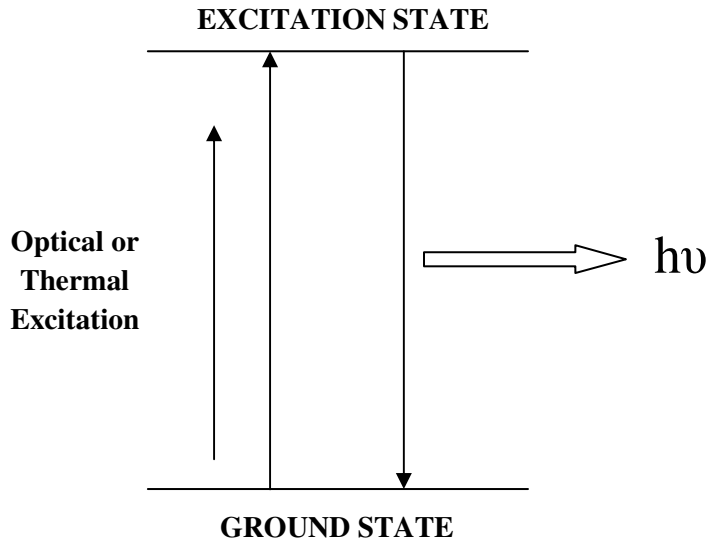


***Figure 1. Origin of Spectra***

## 1.2. ATOMIC ABSORPTION SPECTROSCOPY (AAS):

Atomic absorption spectroscopy uses the absorption of light to measure the concentration of gas-phase atoms. The samples used are generally liquids or solids and the analyte atoms or ions must be vaporized in a flame or graphite furnace. The atoms absorb ultraviolet or visible light and make transitions to higher electronic energy levels. The concentration of the analyte is determined from the amount of absorption. This relationship is defined by Beer's Law:

$$\log_{10} (P_o/P) = A = abc$$

where transmittance [$\log_{10}(P_o/P)$], or absorbance (A), is a function of the constant 'a' specific to the substance, the thickness 'b', and concentration 'c' of the relative number

of absorbers in the light path. According to Beer's law, there is a linear relationship between absorbance (A) and concentration (c) when monochromatic light is used.[3]

$$A \alpha c$$

Concentration measurements are usually determined from a working curve after calibrating the instrument with standards of known concentration.

AAS instruments consist of a light source, atomizers and light separation and detection devices. The light sources that are commonly used are hollow cathode lamps, electrodeless discharge lamps and lasers. AAS requires that the analyte atoms be in the gas phase and samples must be vaporized and converted to atoms in a high temperature source such as a flame or graphite furnace. The light separation and detection systems in AAS include monochromators and photomultiplier tubes (PMT). A schematic of an Atomic Absorption instrument is shown in Figure 2.

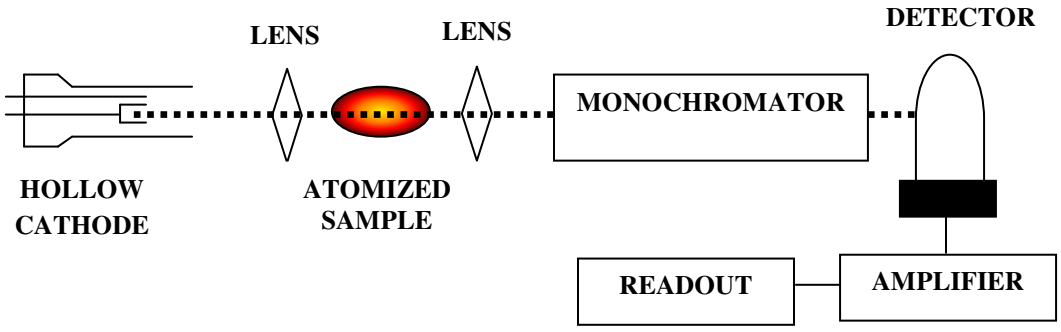


***Figure 2. Atomic absorption spectroscopy***

## 1.3. ATOMIC FLUORESCENCE SPECTROSCOPY (AFS):

Atomic fluorescence involves optical emission from gas-phase atoms that have been excited to higher energy levels by absorption of electromagnetic radiation after which they emit a characteristic fluorescence spectrum. The principle of fluorescence can be illustrated by the schematic diagram shown in Figure 3.

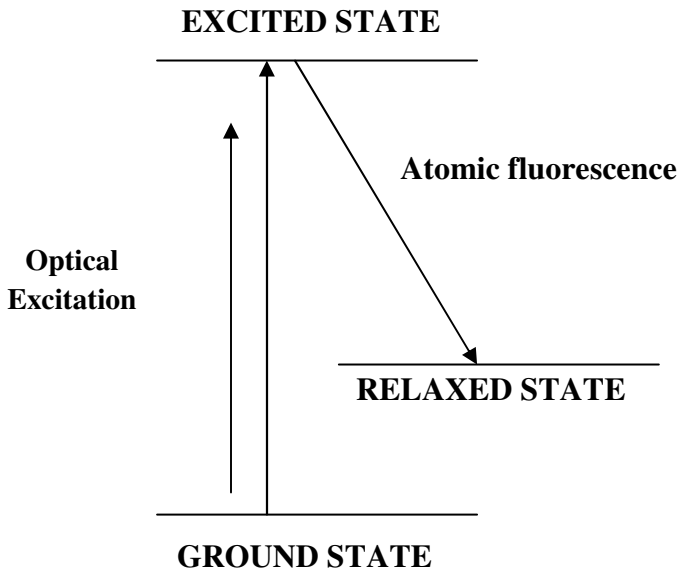


***Figure 3. Schematic representation of fluorescence spectroscopy***

The main advantage of fluorescence measurements compared to absorption measurements is the greater sensitivity that can often be achieved because the fluorescence signal usually has a low background. The resonant excitation also provides selective excitation of the analyte to avoid interferences. The main processes involved in AFS are the creation of free atoms from the sample, absorption of radiation by these free atoms which causes the excitation, and the re-emission of radiation when the atoms return

from the excited state to a lower state. The mathematical expression governing fluorescence intensities have been derived from Beer's Law, which is given by the following expressions:

$$T = I_i/I_o,\ A = -\ln T = abc$$

$$T = e^{-abc}$$

$$I_i/I_o = e^{-abc}$$

$$1 - I_i/I_o = 1 - e^{-abc}$$

Multiplying both sides by $I_o$:

$$I_o - I_i = I_o(1 - e^{-abc})$$

where, $I_o - I_i$ = amount of light absorbed

The basic instrumentation of Atomic fluorescence is similar to that in atomic absorption. The light sources used in fluorescence techniques are usually hollow cathode lamps or lasers. A schematic of atomic fluorescence instrumentation is shown in Figure 4.

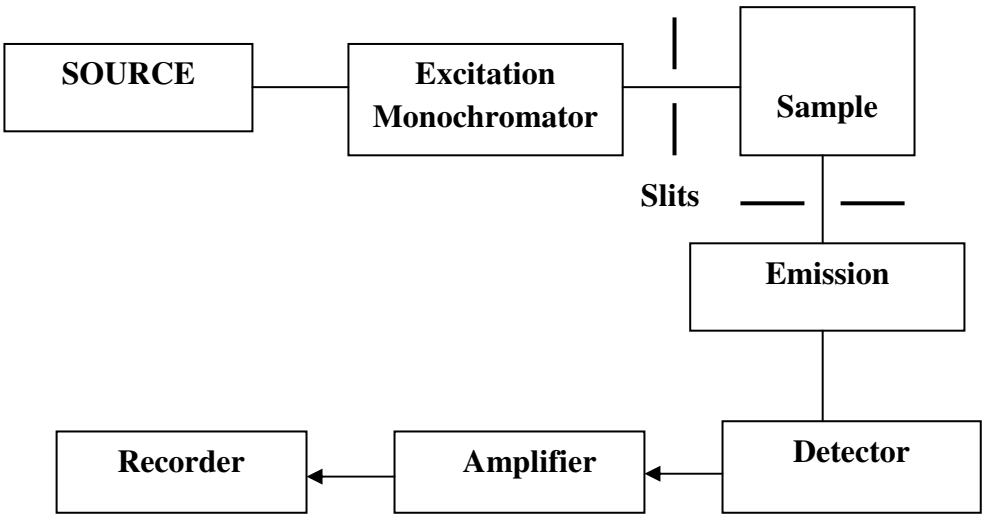


***Figure 4. Atomic fluorescence spectroscopy***

### 1.3.1. LASER INDUCED FLUORESCENCE SPECTROSCOPY (LIFS):

LIFS is one of the atomic fluorescence spectroscopic techniques. Due to the usually low background obtained during analysis, fluorescence techniques are highly sensitive and are often better than corresponding absorption techniques. In LIF, resonant selective excitation of atoms results in reduction of interferences. LIF is useful for the study of the electronic structure of atoms and to make quantitative measurements of analyte concentrations.[4] The excitation source used in LIFS is a tunable laser source.

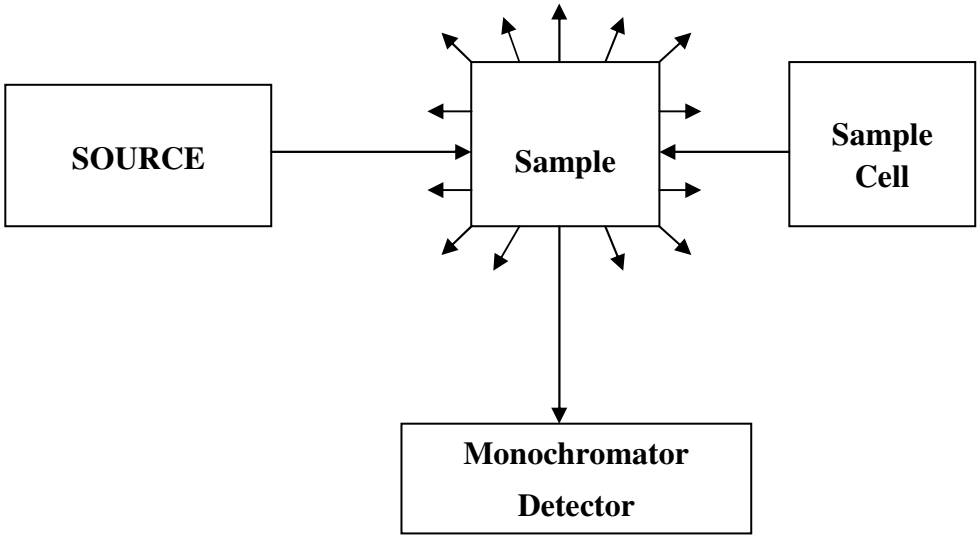


***Figure 5. Laser Induced fluorescence Instrumentation***

The detectors that are commonly used in fluorescence spectroscopy studies are monochromators and photomultiplier tubes (PMT).

## 1.4. ATOMIC EMISSION SPECTROSCOPY (AES or OES):

Plasma Atomic Emission spectroscopy is the study of the radiation emitted by a sample when it is introduced into an electrical discharge. By evaluating the spectra emitted by the plasma, it is possible to determine what elements are present in the sample. Liquids and solids can be analyzed effectively, but gases are more difficult to analyze. All metals and metalloids such as antimony, selenium, and arsenic can be detected in low concentrations but it is difficult to detect non-metals. If mixtures of halides or inert gases are present in the pure gas form, they can be determined directly by the emission spectra generated by an electrical discharge through the gas.[2]

Atomic Emission Spectroscopy (AES or OES) uses quantitative measurement of the optical emission from the excited atoms to determine the concentration of each analyte. Analyte atoms in solution are usually delivered as aerosols into the excited region where they are desolvated, vaporized and atomized. Plasmas are high-temperature atomization sources that provide sufficient energy to promote the atoms into high energy levels. The atoms decay back to lower levels by emitting light. Since the transitions are between distinct atomic energy levels, the emission lines in the spectra are narrow. One of the major advantages of AES compared to Atomic Absorption Spectroscopy (AAS) is that all the analytes are excited and can be detected simultaneously. The different kinds of excitation sources that can be used are:

1. Direct-Current Plasma (DCP)
2. Flame
3. Inductively-Coupled Plasma (ICP)
4. Laser-Induced breakdown (LIBS)

5. Laser-Induced Plasma

6. Microwave-Induced Plasma (MCP)

7. Spark or arc

A schematic of the major atomic emission instrumentation is shown in Figure 6.

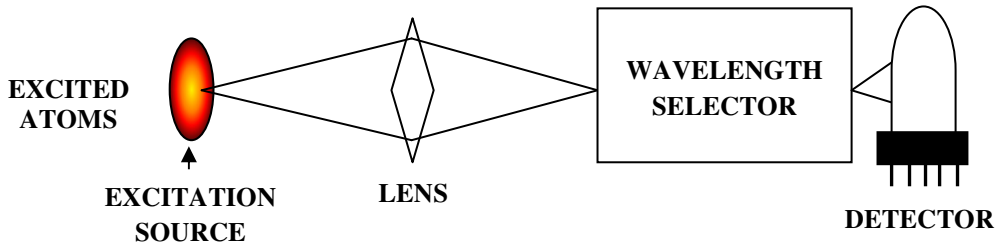


***Figure 6. Atomic Emission Spectroscopy***

The ideal atomic emission atomizer involves the following:

1. Removal of the analyte from its original matrix to minimize interferences.

2. Complete atomization but minimum ionization of the elements to be analyzed.

3. A controllable energy source for excitation, which allows the proper energy needed to excite all elements without appreciable ionization.

4. An inert chemical environment, which avoids the formation of undesirable molecular species that may affect the accuracy of the measurement.

5. No background radiation from the source. Background radiation is any unwanted atomic or molecular emission that could interfere with the analytical wavelengths.

6. A source that can handle a range of solvents, both organic and inorganic in nature.

7. Inexpensive to purchase and maintain.

8. Easy to operate.

### 1.4.1. INDUCTIVELY-COUPLED PLASMA ATOMIC EMISSION SPECTROSCOPY (ICP-AES):

In ICP-AES, the plasma is a partially ionized gas that contains ions, electrons and atoms that is electrically neutral and acts as an atomization and excitation source. The energy maintaining the plasma is provided by an electric or magnetic field. The ICP is produced by coupling the energy from a radiofrequency generator into a gas (usually Argon) via a magnetic field. There are six principal steps involved in the determination of aqueous samples by ICP.[1]

1. Samples are prepared. This may also involve heating, treatment with acids or microwave digestion.
2. Nebulization: Liquids are converted to aerosols.
3. Desolvation/Volatilization: Water is removed and the remaining solids and liquid portions are converted to aerosol.
4. Atomization: Plasma temperature is important for breaking gas phase bonds.
5. Excitation/Emission: Due to collisions, atoms become excited and emit light.
6. Separation/Detection: After the separation of one wavelength with a monochromator the line intensity is measured quantitatively using an optical detector.

A complete ICP-AES instrument consists of a Radiofrequency generator, a coupling unit, a plasma unit with the induction coil, torch, gas supplies and flow controllers, and sample introduction apparatus (usually a nebulizer and spray chamber), imaging optics, a monochromator and detector.[5] The ICP torch consists of three gas flows

(outer loop, intermediate loop and inner loop). The gas flows are delivered through concentric tubes made of silica. The outer loop delivers argon gas at about 15-20 L/min and is the main source of argon for the plasma. The intermediate loop carries auxiliary argon gas at about 200-300 mL/min and is used to raise the plasma up from the lower quartz tube. The inner loop is used to carry the sample into the plasma and the gas flow is typically at a rate of 500-700 mL/min. By adjusting the gas flow rates, one can determine the flow that provides the highest sensitivity for the element of interest.[6] The ICP torch is located inside of a water cooled coil of a radiofrequency generator (r.f). The plasma temperature in the analytical zone ranges from 5000-8000 K and varies with the power and gas flow rates. The plasma efficiently atomizes most samples but also emits a continuum of background radiation that ranges from the visible to the ultraviolet region. The radiation is due to electrons, Ar atoms and $Ar^+$ ions, and various atomic and molecular species. The variation in the continuum background is a major source of noise that ultimately limits the sensitivity of ICP-AES. The different temperature zones in the plasma of an ICP torch are shown in Figure 7.

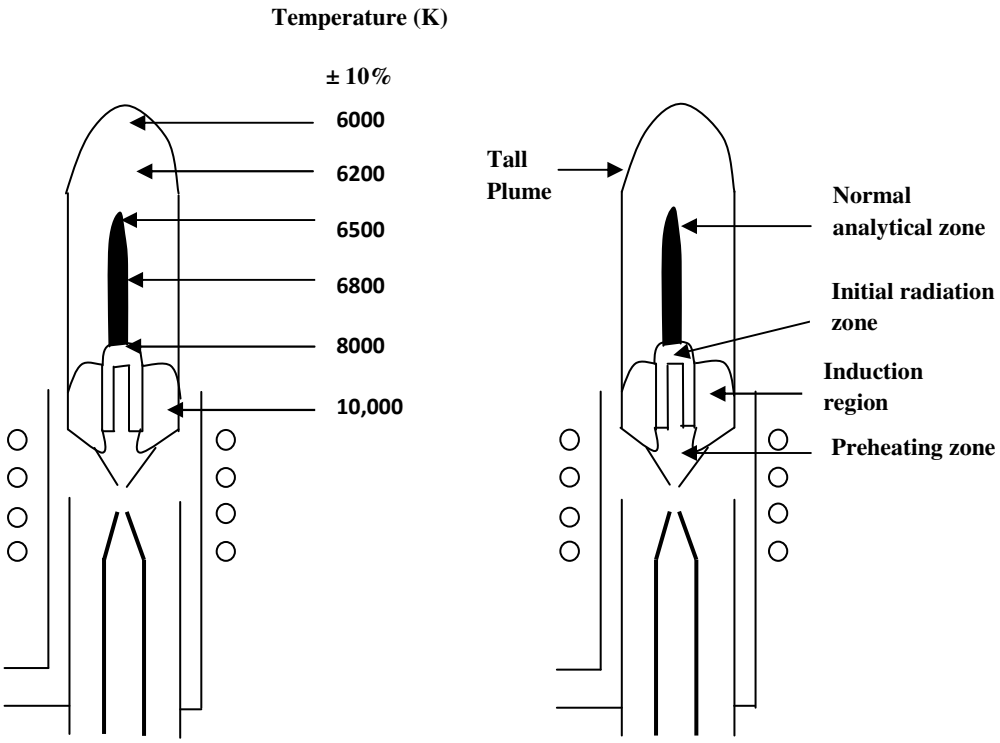


*Figure 7. Different temperature zones in a plasma*

A schematic representation of the ICP torch is shown in Figure 8.

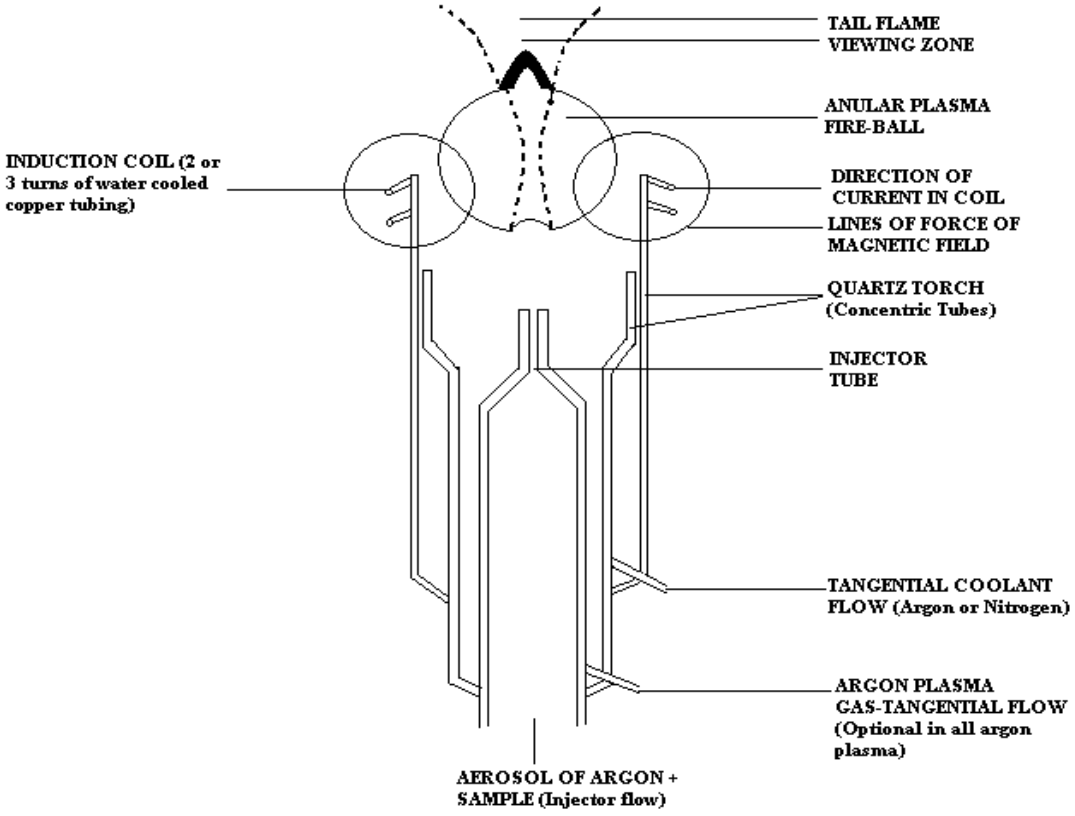


***Figure 8. Schematic of an ICP torch***

A schematic of a typical ICP instrument is shown in Figure 9.

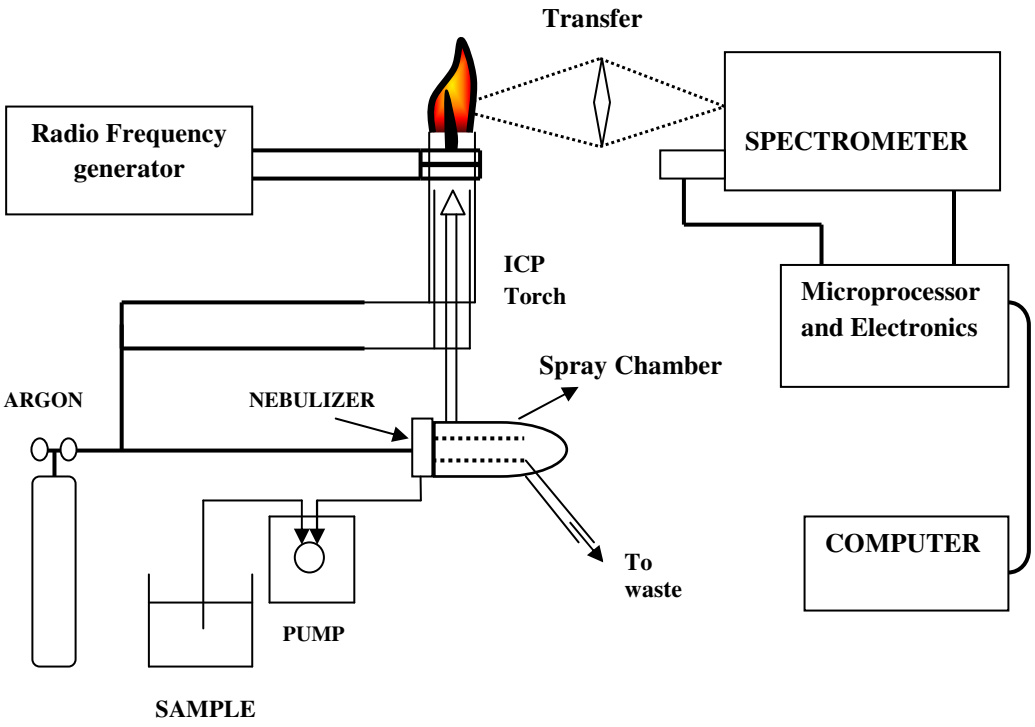


***Figure 9. Schematic of an ICP instrument***

Solution nebulization sample introduction systems are often used for the introduction of the sample into the plasma. The nebulizer uses sample solution at the rate of 1-2 mL/min. The most common samples are cations in solutions including aqueous and non-aqueous samples. Nebulizers are used to convert the liquid sample stream into aerosol, which consists of particles that are 1-10 µm in diameter. There are different kinds of nebulizers used in ICP instruments but the most commonly used one is a pneumatic nebulizer. The other kinds of nebulizers are cross-flow nebulizers, concentric

nebulizers, glass-frit nebulizers, Babington-type nebulizers, V-groove and ultrasonic nebulizers.

The aerosols generated by the nebulizers are carried through spray chambers that are made of glass or inert polymers. The main purpose of a spray chamber is to prevent larger aerosol droplets from reaching the plasma. The gas stream containing the aerosol is guided from the spray chamber through the injector tube which forms part of the quartz torch and then to the base of the ICP.

Atomic emission from the ICP is usually detected with a monochromator and one of several detection devices. The most common detection systems used for the analysis of samples by ICP-AES are monochromators and photomultiplier tubes (PMT).

ICP-AES is useful for measuring nearly all the elements. It is sensitive and accurate with a detection limit of about 1-100 ng/mL for most elements. The major advantage of ICP when compared to other techniques is that multiple elements can be analyzed at the same time.[7] Interferences in ICP-AES can be divided into spectral overlap, stray light, and matrix effects. Spectral interferences are the most common type that is observed and occur when emission lines from two elements are close in energy. The large number of emission lines in the ICP and many potential spectral interference are a significant disadvantage of ICP-AES. Stray light from strong emissions can also contribute to the background at the observed wavelength. Matrix effects can occur either in the plasma or in the sample introduction process.[8]

### 1.4.2. LASER INDUCED BREAKDOWN SPECTROSCOPY (LIBS):

Another type of atomic emission spectroscopy that is being employed in the research is Laser Induced Breakdown Spectroscopy (LIBS). In LIBS, the vaporizing and exciting plasma is produced by a high-power focused laser pulse. Pulses from the laser are focused on the sample using a lens and the plasma light is collected using a second lens. The light that is collected is transported to a wavelength selection device and then detected. Each laser pulse produces a single LIBS measurement. Since the laser plasma is transient, time resolution of emissions from the spark may improve the signal-to-noise ratio and discriminate against interferences.

The plasma formed in LIBS differs from that formed in conventional ICP-AES in two important ways. Firstly, the LIBS plasma is non-continuous whereas that formed in an ICP-AES is continuous. Secondly, delays and widths in the plasma emission decay process can be measured in LIBS, which is not possible in an ICP-AES instrument. The majority of LIBS measurements are performed using a RSS (Repetitive Single Spark) in which a series of individual laser sparks are formed at the laser repetition rate (e.g. 10 Hz). Sometimes to enhance the detection capabilities, a RSP (Repetitive Spark Pair) is used where a series of two closely spaced sparks (1-10 μs separation) are used.[9]

The components of a LIBS system include an excitation source (a laser), a sample cell where the plasma is produced, a sample container and a detection system. The laser that is most commonly used as an excitation source is the Nd: YAG laser due to its reliability and ability to produce powerful laser pulses. The spectrally resolved signal can be detected with a photomultiplier tube (PMT), photodiode array (PDA), and charge-

coupled device (CCD) or charge injection device (CID).[10] A schematic of the basic laser induced breakdown apparatus is given in Figure 10.

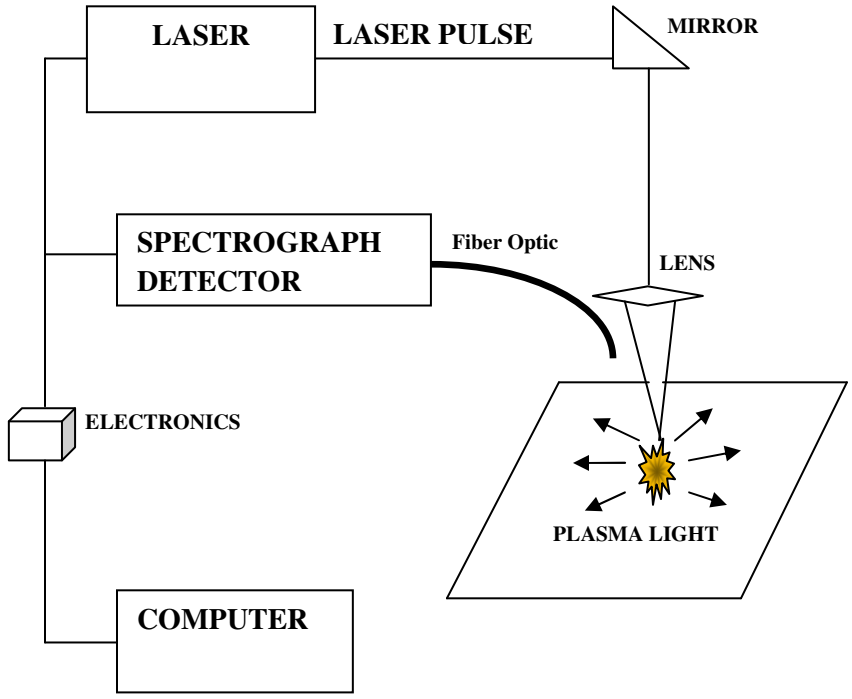


***Figure 10. Laser Induced Breakdown Spectroscopy***

There are several advantages in using LIBS. The major advantage is that LIBS can be used for remote sensing and process monitoring as the sample only requires optical access. In addition, the sample used for analysis in LIBS does not need to be transported to the plasma source as the plasma is formed within the sample or at the surface of the sample. Only a very small amount of the sample is used and atomization and excitation are a single step process in LIBS. Disadvantages of LIBS include poor

detection limits when compared to ICP-AES, poor precision which is around 5-10% and complexity.[11]

## 1.5. LASER SYSTEM:

The light source used in LIF and LIBS spectroscopy methods is a laser (Light Amplification by Stimulated Emission of Radiation). A typical laser emits a narrow, low-divergence beam which has a narrow wavelength spectrum. The laser that has been used in this research is a Nd: YAG laser. A typical Nd: YAG laser configuration is given in Figure 11.

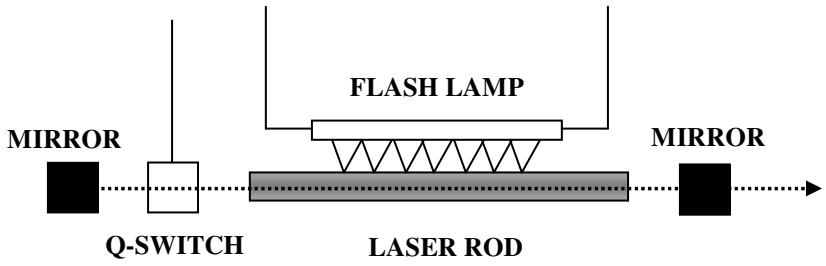


***Figure 11. Nd: YAG Laser configuration***

Nd: YAG lasers are often used as they are reliable, compact, provide high power laser pulses and are easy to use. The fundamental wavelengths in a Nd: YAG laser can also be converted to generate pulses at fixed wavelengths ranging from the near IR to the near UV spectral regions. Different harmonic wavelengths are often produced by passing the laser light through a birefringent material such as potassium dihydrogen phosphate (KDP) or potassium dideuterium phosphate (KD*P) crystals. The fundamental wavelength of the Nd: YAG laser is 1064 nm which can be converted to 532 nm (2$^{nd}$

harmonic). The third harmonic of 355 nm is generated by combining the residual 1064 nm light with converted 532 nm. Radiation at 266 nm or $4^{th}$ harmonic is produced by doubling the 532 nm light.[12]

The energies of the fundamental and harmonic wavelengths of the Nd: YAG laser are given in Table 1.

| WAVELENGTH (nm) | ENERGY (mJ) |
|---|---|
| 1064 | 650 |
| 532 | 270 |
| 355 | 170 |

***Table 1. Energies of Nd: YAG laser at different harmonics***

### 1.6. DETECTORS:

Different kinds of detectors are used for detection in atomic spectroscopic techniques.

#### 1.6.1. PHOTOMULTIPLIER TUBE (PMT):

A PMT consists of a photo sensitive cathode and a series of dynodes that are set at increasingly positive potentials until an anode is reached. Light coming from the plasma source passes through the window of the PMT and hits the cathode. This causes the emission of photo-electrons which are accelerated towards the first dynode. Each time an electron impacts with a dynode, a number of secondary electrons are emitted. This causes an avalanche of electrons which amplifies the signal effectively (by a factor of $10^6$). The

cathode in a PMT is coated with a semi-conductive material which is easily ionized, such as alloys of alkali metals with antimony, bismuth and/or silver.[13] Gallium-arsenide is a common material that has a fairly constant response over a wide wavelength range. Other common materials are cesium-antimony or sodium-potassium-cesium-antimony compounds.[14]

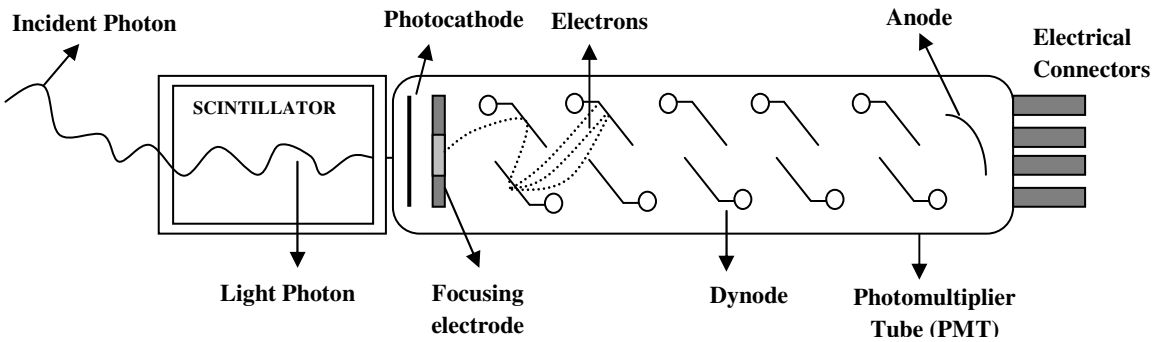


***Figure 12. Photomultiplier tube (PMT)***

### 1.6.2. MONOCHROMATOR:

A monochromator is an optical device that transmits a specific band of wavelengths of light. It consists of a diffraction grating, slits, and mirrors. Typical uses are the isolation of a narrow band of radiation from a continuum light source or the analysis of the emission from excited atoms or molecules. A schematic representation of a monochromator used for analysis of radiation is shown in Figure 13.

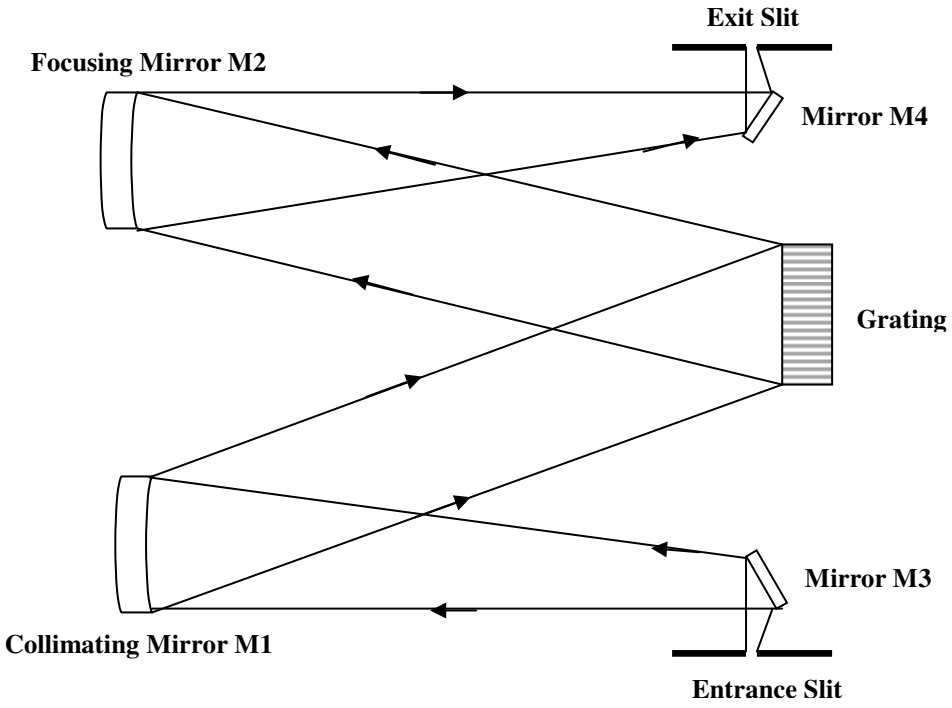


***Figure 13. Monochromator***

Sequential monochromator systems allow for the analysis of only one analytical wavelength at a time, which is time consuming. To scan an entire region of the electromagnetic spectrum with a sequential system, the detector is held at a fixed position and the grating is turned. More efficient systems that can measure specific wavelengths at multiple positions simultaneously are called polychromators.

In addition to PMTs, the other types of detectors are one-dimensional solid state detectors and are know as Photodiode arrays (PDA). The PDA is similar to a PMT in that the detectors are in a fixed position, but the PDA detectors are much smaller and are positioned in a linear array. As a result, many more detectors can be used in a single instrument. A typical PDA will hold 1,024 miniature detectors that measure energy

simultaneously over a two- to three-inch distance. Depending on the monochromator, this allows spectral windows of 50–100 nm to be simultaneously measured.

A charge coupled device is an example of a two dimensional light detector. A CCD allows multi-element analysis using more than one wavelength per element. Each detector element (or pixel) accumulates a charge proportional to the light energy striking it. A CCD commonly uses a grating with a prism to disperse the wavelengths of light in two dimensions.[1]

In each case, the radiation detector produces an electric signal that is processed by a circuit before it is registered by a read-out device. The electronic circuit amplifies the signal and converts it to a digital signal before it is acquired by a computer.[14]

## 1.7. CALIBRATION ANALYSIS:

After the analysis of a sample using spectroscopic techniques, the data are often collected and plotted with the signal or intensities on the y-axis and the concentration on the x-axis. Plotting a calibration curve allows the determination of the concentration of a substance in an unknown sample by comparing the unknown to a set of standard samples of known analyte concentrations.

The limit of detection (LOD) is the lowest quantity of a substance that can be distinguished from a blank value with a stated degree of confidence. It can also be defined as the smallest amount of analyte that produces a signal.[15] The LOD is determined from the mean of the blank, the standard deviation of the blank and some confidence factor.

Limit of Detection is calculated in these studies by the following expression:

$$\mathbf{LOD = \frac{3 * \sigma}{m}}$$

where, σ = Standard Deviation of the blank

m = Slope of the calibration curve

The LOD is expressed in units of concentration (ppb, ppm).

# CHAPTER 2: ANALYSIS OF METALS

## 2.1. ANTIMONY:

Antimony and its compounds have been listed as priority pollutants by the Environmental Protection Agency of the United States (US-EPA) and the European Union.[67] Antimony species in the environment include both inorganic and organic forms. The toxicity of antimony depends on the chemical forms of the element. Inhalation exposure to antimonials has been reported to produce pneumonitis, fibrosis, bone marrow damage and carcinomas.[16] The US-EPA has recommended 0.006 mg/L as a limit in drinking water. Antimony enters the aquatic environment as a result of the weathering of rocks, from solid runoff, through effluents from mining and manufacturing, and from municipal discharges. Weathered rocks contain an average of 0.16 ppm Sb.[17] Inorganic species of antimony are more toxic than methylated ones, and Sb(III) is 10 times more potent than Sb(V).[67] The two common inorganic forms of antimony present in natural waters are antimonate ($Sb(OH)_6^-$) and antimonite ($Sb(OH)_3$). Antimony is considered a non-essential element and toxic to most organisms at higher concentrations.[18]

The measurements of total element concentrations without distinguishing the various forms in which it is present do not provide complete information about their mobility, bioavailability, toxicity or environmental behavior,[19] so analytical methods such as chromatographic separations combined with element-specific detectors (atomic spectrometry) have been developed for their detection. The analytical techniques used to study volatile antimony species previously include Gas chromatography (GC) coupled to atomic absorption spectrometry (AAS), mass spectrometry (MS) or inductively coupled

plasma mass spectrometry (ICP-MS). High performance liquid chromatography (HPLC) coupled with hydride generation atomic absorption spectrometry (HG-AAS), hydride generation atomic fluorescence spectrometry (HG-AFS), inductively coupled plasma atomic emission spectrometry (ICP-AES) are also widely used techniques for speciation of soluble antimony species.[20]

Most of the work previously done in this area used HPLC coupled to hydride generation atomic absorption spectrometry (HG-AAS), hydride generation atomic fluorescence spectrometry (HG-AFS) or hydride generation inductively coupled plasma emission spectrometry (HG-ICPES). Research has also been done to compare continuous flow hydride generation laser-induced fluorescence and laser-enhanced ionization spectrometry to measure parts per trillion levels of arsenic, antimony and selenium species and it was found that the limits of detection for arsenic and antimony were 200 and 300 fg/mL respectively, using HG-LIF.[21]

In this research, the detection of antimony species in aqueous samples using HG-LIF has been studied in an attempt to compare the detection limits obtained from other techniques such as inductively coupled plasma atomic emission spectroscopy (ICP-AES) and hydride generation sample introduction combined with LIBS detection.

**2.2. SELENIUM:**

Selenium is an important trace element that is essential for human health as it is involved in the formation of at least 13 proteins and is a component of the glutathione peroxidase enzyme.[22] It is an essential element at low concentration but can be a toxic element at higher concentrations.[23] The bioavailability, toxicity and chemoprotective

activity of selenium depends on its form.[24] Different selenium species are absorbed in a different manner by the human body and have different tendencies to bioaccumulate. As a result, selenium speciation is important for understanding its effects.

The maximum allowable concentration of selenium in drinking water according to US-EPA and in Canada is 10 µg/L.[68, 25] Incidents of acute selenium toxicity to livestock have been reported, but chronic exposures are the primary concern for humans.[26] The level of selenium in air ranges from 0.1 to 10 ng/m$^3$ and levels of selenium in groundwater and surface water range from 0.06 to about 400 µg/L but can reach 6000 µg/L.[27] Recommended daily intakes have been set at 1.7 µg/kg of body weight in infants and 0.9 µg/kg of body weight in adults.[28] Long term exposure to high levels of selenium may lead to teratogenicity, reproductive toxicity and embryotoxicity. Selenium also has carcinogenic effects on humans. Recent studies have also indicated that selenium supplementation may provide cancer-protective benefits in humans.[29]

Atomic absorption spectrometry with hydride generation is a common method of determining selenium in drinking-water. If 10 mL samples are used for routine analysis, the detection limit is about 0.5 µg/L. Lower levels can be determined if larger sample volumes are used.[30] It has been demonstrated that when HG is coupled with ICP-AES/MS, the detection limits of selenium and other hydride-forming elements are improved by 10–100 times.[31] Speciation of selenium is mostly carried out using liquid chromatographic (LC) techniques, such as ion-pair, ion-exchange and size exclusion chromatography coupled with inductively coupled plasma-mass spectrometry (ICP-MS)[32], flame atomic absorption spectrometry (AAS)[33], hydride generation atomic fluorescence spectrometry (HG-AFS)[34] and inductively coupled plasma-atomic emission

spectrometry (ICP-AES).[26] However these methods may not be sufficiently sensitive for the direct determination of Se because they provide detection limits between 10 and 100 ng/L.[35] As a result, many HG-AFS, HG-AAS and HG-AES methods involve preconcentration procedures, based on ion-exchange,[36] coprecipitation,[37] solvent extraction[69] and hydride trapping with a graphite furnace[38] or by cryogenic methods,[39,40] to improve their detection limits.

In this research, the detection of selenium was carried out using hydride generation coupled to inductively coupled plasma emission spectroscopy (HG-ICPES) and hydride generation coupled to laser induced breakdown spectroscopy (HG-LIBS). Speciation of Se was also investigated using the LIBS technique.

The other elements that were analyzed during this research were Aluminium (Al), Manganese (Mn) and Iron (Fe). These elements were analyzed using atomic emission spectroscopic methods by means of direct nebulization.

**2.3. ALUMINIUM:**

Aluminium is considered to be a nonessential and toxic element for living organisms that accounts for approximately 8.3% of the earth's crust and is found in air, water, plants and food.[41] High concentrations of aluminium in soil and natural waters are considered to be poisonous to plants, fish and marine organisms[42] Certain human illnesses, may be caused due to aluminium exposures.[43,44] The amount of aluminium allowed in drinking water according the US-EPA is 0.05 to 0.2 mg/L. Aluminium can occur in food products by leaching from cookware or storage containers when the

contents are acidic. It is also a component of food additives and is used during water treatment process.[45]

The concentration of Al in biological samples is low when compared to other natural samples. Humans are frequently exposed to Al by the intake of Al containing drugs, inhalation of atmospheric dust and dietary sources. Al has been reported to be a factor in several diseases, particularly in patients with chronic renal failure.[47] Elevated levels of Al in humans may lead to Alzheimer's disease, Parkinson's disease, Parkinson-Guam's disease, amyotrophic lateral sclerosis, diabetes and cancer.[48]

Several techniques have been employed in the detection of Al in water samples. The most commonly employed technique is inductively coupled plasma emission spectrometry/mass spectrometry (ICP-AES/MS) because of its capability for multi-element detection over a wide concentration range with relatively low detection limits. In this research, inductively coupled plasma atomic emission spectroscopy (ICP- AES) has been employed for the detection of Al.

**2.4. IRON (Fe):**

Iron is one of the most important elements in biological systems and is widely distributed in nature. Chemical properties such as valence, solubility, and the degree of chelation or complex formation influence the biological activity of iron.[49] At low concentrations, iron plays an important role in fermentation processes and metabolism.[50] Deficiency of iron may lead to reduced hemoglobin synthesis and anemia. Iron is mostly detected by using flame and graphite furnace atomic absorption spectrometry.[51]

In this research, inductively coupled plasma atomic emission spectroscopy (ICP-AES) has been employed for the detection of Fe.

## 2.5. MANGANESE (Mn):

Manganese is both an essential and a neurotoxic trace element that plays a role in bone and tissue formation, and the activation of many enzymes that are involved in metabolic processes and reproductive functions. Since dietary sources generally provide adequate amounts of Mn (2-8 mg) per day, deficiency is not common with this element. Exposure to Mn in urban environments may increase due to the use of a manganese-containing compound in gasoline.[52] Exposures may lead to Parkinson-like symptoms and may cause impotency. The most frequently used spectroscopic techniques for measuring Mn include inductively coupled plasma mass spectrometry (ICP-MS) and atomic absorption spectrometry (AAS).

In this research inductively coupled plasma atomic emission spectroscopy (ICP-AES) has been employed for the detection of Mn.

# CHAPTER 3: GOAL OF THE PROJECT

Antimony and Selenium are environmentally important trace elements. The development of an improved method for the speciation of antimony and selenium species would allow effective measurements of different forms of these elements. The long term goal of this project is to develop methods to speciate these elements at low concentrations. High Performance Liquid Chromatography will be the method employed to separate the species as this method is the most widely method used for speciation in a variety of samples. HPLC with atomic spectrometry detection will be used as this approach is sensitive and selective for the speciation analysis. This approach will be used as it generally does not require complicated derivatization steps of the analytes to achieve their separation prior to determination.[20,53-56] In this project, studies have been performed to evaluate different detection approaches using hydride generation (HG) coupled to laser induced fluorescence spectrometry (LIF), inductively coupled plasma emission spectrometry (ICP-AES) or laser induced breakdown spectrometry (LIBS).

# CHAPTER 4: MATERIALS AND METHODS

## 4.1. LASER INDUCED FLUORESCENCE (LIF):

### 4.1.1. LASER SYSTEM:

The main component used for the Laser Induced Fluorescence studies is an Nd: YAG laser (Surelite SL-II10, Continuum). This laser has a pulse width of 7-8 ns and it operates at a frequency of 10 Hz. This laser also serves as a pump source for a dye laser (Northern Lights). The dye used in the dye laser was 0.25 g of Stilbene dissolved in 1000 mL methanol. The light from the laser passes through a nonlinear crystal which produces tunable ultraviolet radiation by means of frequency doubling. The UV light of required wavelength is isolated by passing the laser beam through a quartz Pellin-Broca prism.

### 4.1.2. HYDRIDE GENERATION APPARATUS (HG):

The Hydride Generation (HG) system is a continuous flow sampler and is used to convert the metal or metalloid atoms into gaseous hydrides. The HG system consists of a four channel peristaltic pump (Dynamax Peristaltic pump, Rainin Instrument Co. Inc.,), a gas-liquid separator (GLS) and a nafion tube dryer. The peristaltic pump delivers the sample solution, $NaBH_4$, and HCl at a constant rate of 15 r.p.m. The flow rates of the solution through the tubing can be controlled by adjusting the speed of the peristaltic pump. The tubing used was about 1-2 m in length and had an internal diameter of about 1-3 mm. The amount of sample that was delivered to the hydride generator was around 8 mL/min. The flow rates of each solution though the peristaltic pump was controlled by using pump tubing with various diameters. This solution is carried to a gas liquid

separator (GLS) which is made of pyrex glass. A schematic of the HG apparatus is shown in Figure 14.

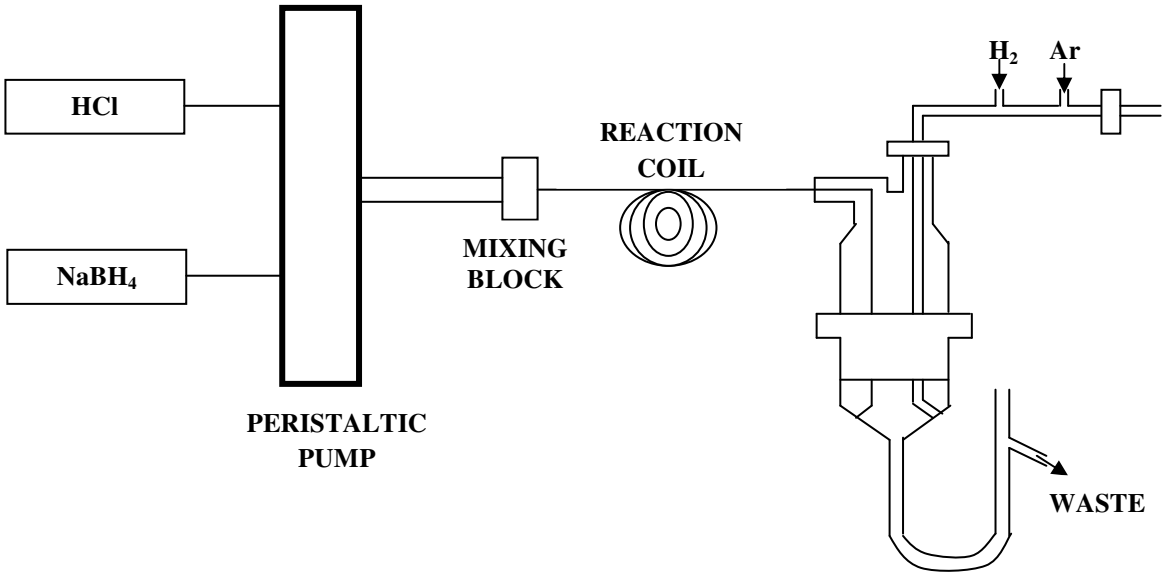


*Figure 14. Hydride Generation Apparatus*

#### 4.1.2.1. SODIUM TETRAHYDROBORATE ACID REDUCTION SYSTEM:

The reaction system that is being used for the production of hydrides inside the hydride generation apparatus is based on the generation of hydrogen in the reaction of $NaBH_4$ with acid.[58]

$$NaBH_4 + 3H_2O + HCl \longrightarrow H_3BO_3 + NaCl + 8H^{\bullet}$$

$$8H^{\bullet} \xrightarrow{E^{m+}} EH_n + H_2 \text{ (excess)}$$

where, E is the analyte element and m may or may not be equal to n.

### 4.1.3. DETECTION:

In the LIF experiments, the wavelength of absorption for antimony was found to be 212.739 nm and was set accordingly on the dye laser (Spectra Drive). Likewise, the wavelength of emission was found to be 259.8 nm and was set on the monochromator (Acton Research Corporation Spectra Pro-275). The monochromator was connected to a photomultiplier tube (PMT) where the fluorescence signal was detected. The PMT was set to a voltage of -1200 V and the monochromator slit width was adjusted to 1500 μm. Neutral Density (ND) filters were used during the measurement of antimony by LIF techniques. The purpose of these filters was to attenuate the light reaching the monochromator. The light passing through the monochromator was detected by the PMT that was connected to a Boxcar averager or integrator which in turn was connected to the computer. Helium and Argon gases were used during the measurements and the flow rates were adjusted to 10 and 30 sccm, respectively. A schematic diagram of the laser induced fluorescence apparatus is given in Figure 15.

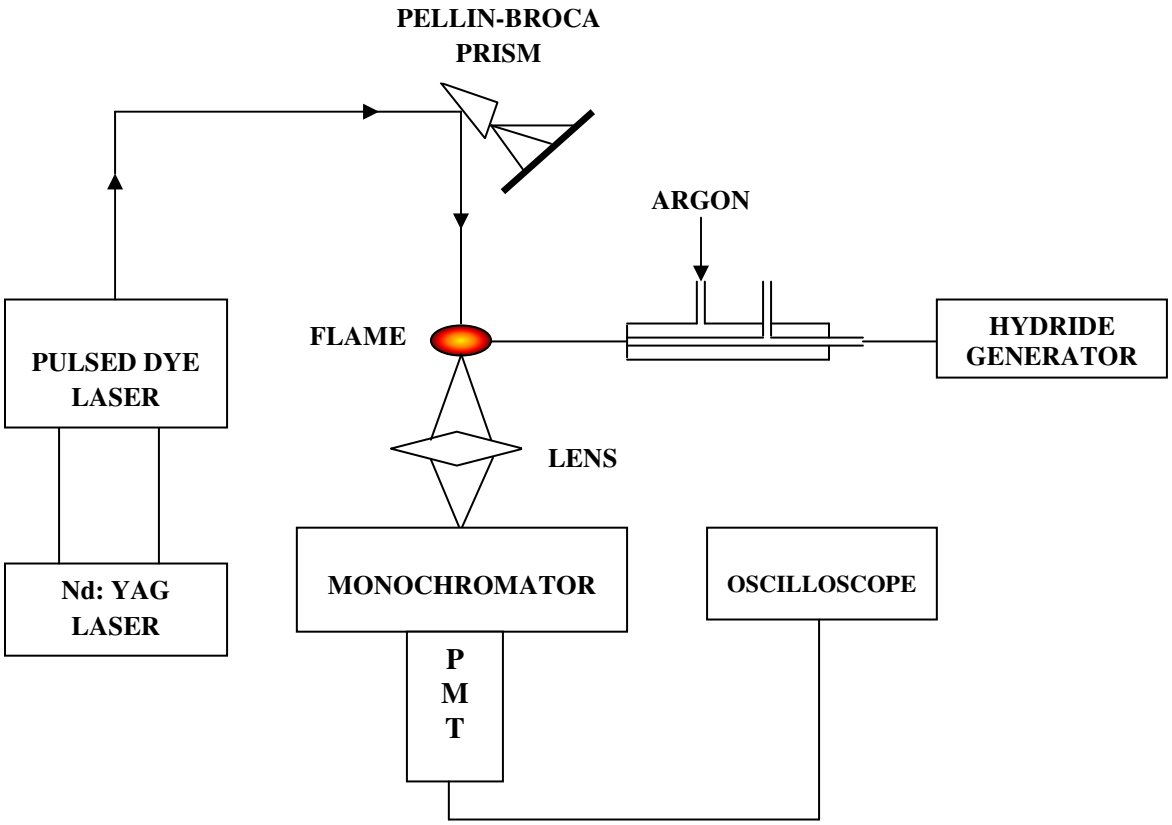


***Figure 15. Hydride generation Laser Induced Fluorescence Apparatus (HG-LIF)***

## 4.2. INDUCTIVELY-COUPLED PLASMA ATOMIC EMISSION SPECTROSCOPY (ICP-AES):

The ICP employed for these experiments was an ARL 3410 ICP with Minitorch. The hydride generator apparatus was connected to the ICP with tubing that delivered the hydride gases from the HG to the base of the ICP torch. For some experiments, samples were introduced by solution nebulization. The nebulizer converted the sample solution to aerosols. Argon gas was used for the production of plasma and the pressure of the gas was controlled at 30 psi. Another argon gas cylinder was used to control the flow of the

sample into the nebulizer and its pressure was maintained at 30 psi. The main purpose of the plasma was to atomize and excite the sample metal species coming through the nebulizer.

### 4.2.1. HYDRIDE GENERATION APPARATUS (HG):

The Hydride Generator apparatus used in the ICP-AES measurement was the same as that used in the LIF studies. The sample, sodium borohydride ($NaBH_4$) and hydrochloric acid (HCl) solutions were pumped via the peristaltic pump into the mixing chamber and gas liquid separator to produce the hydride which was delivered directly to the torch. The tubing dimensions used were similar to that used in the LIF technique and the flow rate was also the same.

### 4.2.2. METHOD DEVELOPMENT:

In the ICP-AES approach, the monochromator was calibrated with the blank solution. Line location was performed for metals of interest and the wavelength at which the line was located for each element was noted. A method was developed to perform a calibration for different concentrations of the metal at the detected wavelength. The emitted light of the desired wavelength was allowed to pass through the monochromator and was further detected by means of a photomultiplier tube (PMT).

### 4.2.3. DETECTION:

Sb and Se were detected using the hydride generation coupled with inductively coupled plasma emission spectroscopy (HG-ICP-AES). Different wavelengths of

emission were located for these elements and the best wavelength where maximum signal was observed was 217.575 nm and 196.090 nm for Sb and Se, respectively. The flow rate of the peristaltic pump was set to 15 r.p.m and the flow rate for the Ar gas used to calibrate the monochromator was set at 10 sccm and that used to aid the flow of the sample from the HG was set at 40 sccm. The integration time was set to 5 sec. Elements such as manganese (Mn), aluminium (Al) and iron (Fe) were also detected using the ICP, but without the hydride generator. The wavelength of emission for these elements was found to be 293.268 nm, 394.379 nm and 273.933 nm respectively. Calibration for Sb was performed using a concentration of 0.03, 0.1, 0.3, 1, and 3 ppm. Calibration for Se was performed using a concentration of 0.03, 0.1, 0.3, 1, 3, and 10 ppm. The concentrations of sodium borohydride ($NaBH_4$) and hydrochloric acid were optimized to get the best calibration curve. A schematic of the HG-ICP-AES is shown in Figure 16.

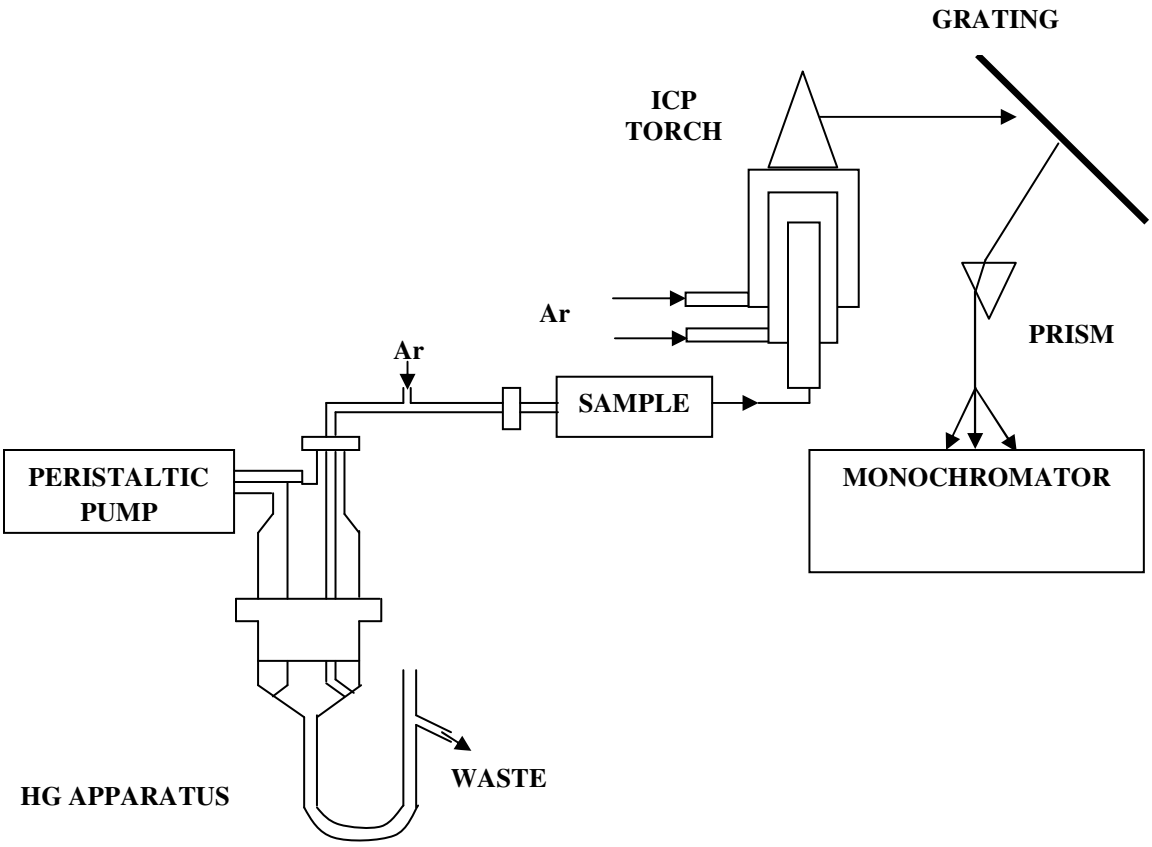


***Figure 16. Hydride Generation Inductively Coupled Plasma Atomic Emission Spectroscopy apparatus***

## 4.3. LASER INDUCED BREAKDOWN SPECTROSCOPY (LIBS):

### 4.3.1. LASER SYSTEM:

The laser system used in LIBS is the same as that used in the LIF technique. A Nd: YAG laser (Surelite SL-II10, Continuum) was operated at a frequency of 10 Hz. The light coming out of the laser is directed towards a Pellin- Broca prism. The LIBS technique is different from the LIF technique in two aspects. Firstly, a dye laser is not used in LIBS detection and secondly a plasma instead of a flame is employed as an

atomization source. This plasma is produced in a flow of Ar gas. This Ar gas also aids in the flow of the hydride gases from the peristaltic pump into the HG apparatus.

### 4.3.2. HYDRIDE GENERATION APPARATUS:

The HG apparatus used in the LIBS studies was the same as that used in the previous studies involving LIF and ICP-AES. The sample, sodium borohydride ($NaBH_4$) and hydrochloric acid (HCl) solutions were pumped via the peristaltic pump into the gas liquid separator to produce the hydride which was delivered directly to the plasma formed by the laser. The tubing dimensions used were similar to that used in the LIF technique and the flow rate was also the same.

### 4.3.3. DETECTION:

Various scans were performed using a 10 ppm Se solution to find the best wavelength where maximum emission occured and this wavelength was found to be 196.1 nm. The wavelength of the monochromator was set and the plasma emission was detected using a PMT whose voltage was set at -1200 V. The Boxcar averager (SRS, Ortec 400 1M Minibin and power supply) was adjusted to different delays, width and averaging. Different delays from 100 ns to 9 µs were evaluated to optimize the response. The widths were adjusted from 1 µs to 3 µs. The maximum signal for Se was observed at a delay ($t_d$) of 700 ns, width ($t_w$) of 3µs and the averaging was changed from 30 to 1000. Initially the monochromator slit width was adjusted to about 20-30 µm and the calibration for different concentrations of Se (1, 2, 5, 7, 10, and 15 ppm) was performed. The concentrations of $NaBH_4$ and HCl that were used to perform the calibration were

1.5% $NaBH_4$ with 0.4% NaOH and 10% HCl. A schematic of the HG-LIBS apparatus is shown in Figure 17.

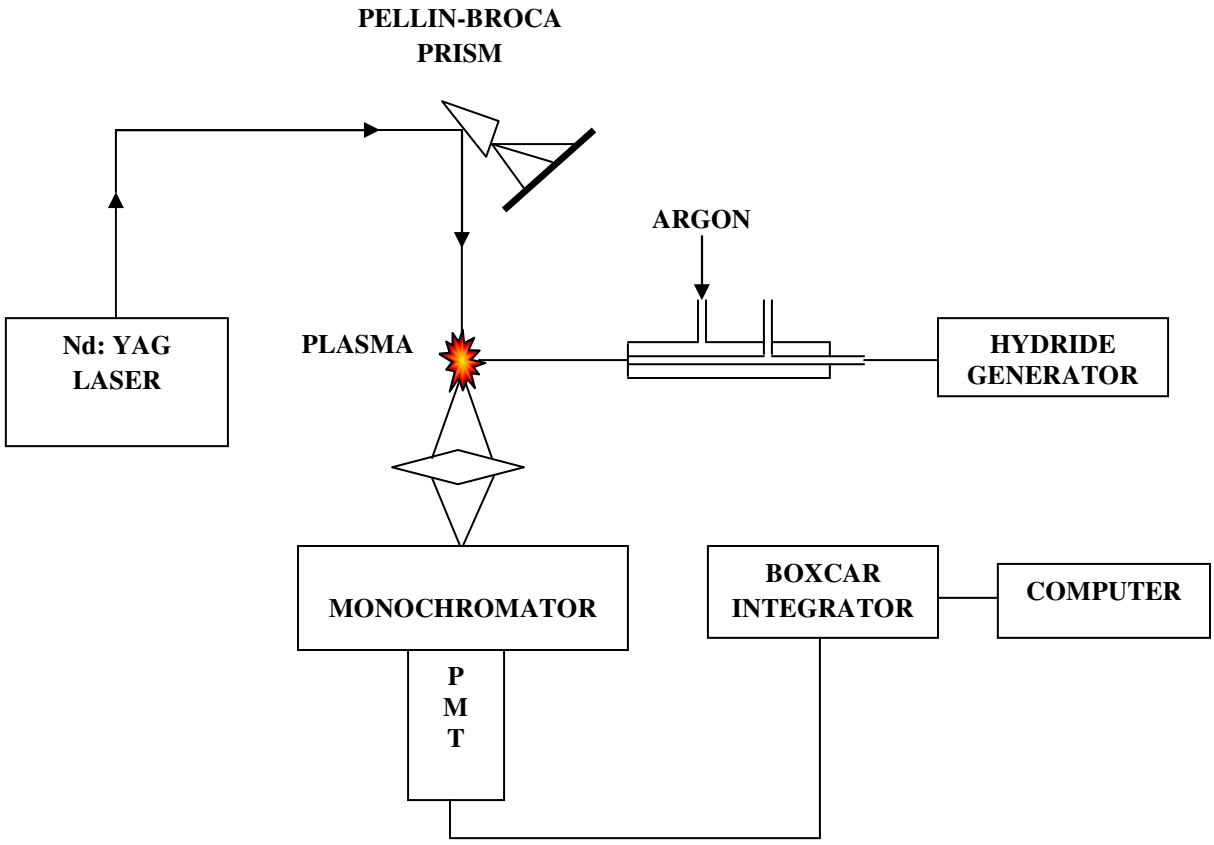


***Figure 17. Hydride Generation Laser Induced Breakdown Spectroscopy (LIBS) apparatus***

## 4.4. REAGENTS AND STANDARDS:

Standard Reference stock solutions of Se (1000 ppm ± 1%, Fisher Scientific), Sb (Atomic absorption standard solution, Aldrich), Mn (1000 ppm ± 1%, Fisher Scientific), Fe (1000 ppm ± 1%, Fisher Scientific), and Al (1000 ppm ± 1%, Fisher Scientific) were used to prepare calibration standards by means of serial dilution using de-ionized water obtained from the laboratory. The standard solution contained a small amount of HCl to stabilize the pH of the solution.

All acid solutions were prepared using de-ionized water obtained from the laboratory. $NaBH_4$ (AF granules, 10-40 mesh, 98%, Sigma Aldrich) was used to prepare the borohydride solution. A 1.5% borohydride solution was prepared by dissolving 3.75 g of $NaBH_4$ in 250 mL of de-ionized water and was stabilized by adding 0.4% m/v of NaOH pellets (Fluka). The 10% acid solution was prepared by dissolving 67.5 mL of concentrated HCl (35%-38% v/v, Pharmaco Aaper) in 182.5 mL of de-ionized water.

Different concentrations of $NaBH_4$ and HCl solutions were prepared during the experiment to optimize the instrument by dissolving different amounts of borohydride and HCl in de-ionized water. On-line hydride generation was achieved by mixing 1.5% $NaBH_4$ in 0.4% NaOH and 10% HCl. The intensity of emission obtained was plotted against the concentration of sample metal solution to determine the slope of the curve and the limit of detection was calculated.

For speciation analysis, a buffered solution of TRIS (Hydroxymethyl amino methane) (Certified A.C.S. Fisher Scientific) was used. Solutions with different pH's were prepared by adjusting the pH with concentrated HCl. In speciation analysis, with

HG-LIBS, the HCl solution normally used with $NaBH_4$ was replaced with TRIS and the responses were observed.

Ethyl alcohol ($C_2H_5OH$; 200 proof, anhydrous, 99.5 +%) was used for the ethanol enhancement studies with Se using HG-LIBS. Different concentrations of ethyl alcohol were added to 10 ppm solution of Se and the responses were plotted against the % of ethyl alcohol added.

# CHAPTER 5: RESULTS AND DISCUSSION

## 5.1. LASER INDUCED FLUORESCENCE (LIF) STUDIES:

Laser induced fluorescence (LIF) studies were carried out to evaluate the analytical performance of a hydride generation-LIF approach for measuring antimony in aqueous samples.

### 5.1.1. SPECTRUM OF ANTIMONY:

In order to determine the best fluorescence emission wavelength, a fluorescence emission spectrum was obtained. A 10 ppb solution of antimony was used to obtain the fluorescence spectrum and the wavelength of the laser was set at 212.739 nm. The strongest fluorescence wavelength was found to be 259.805 nm. The peak at 212.7 nm observed in the fluorescence spectrum was due to the scattering of light from the laser.

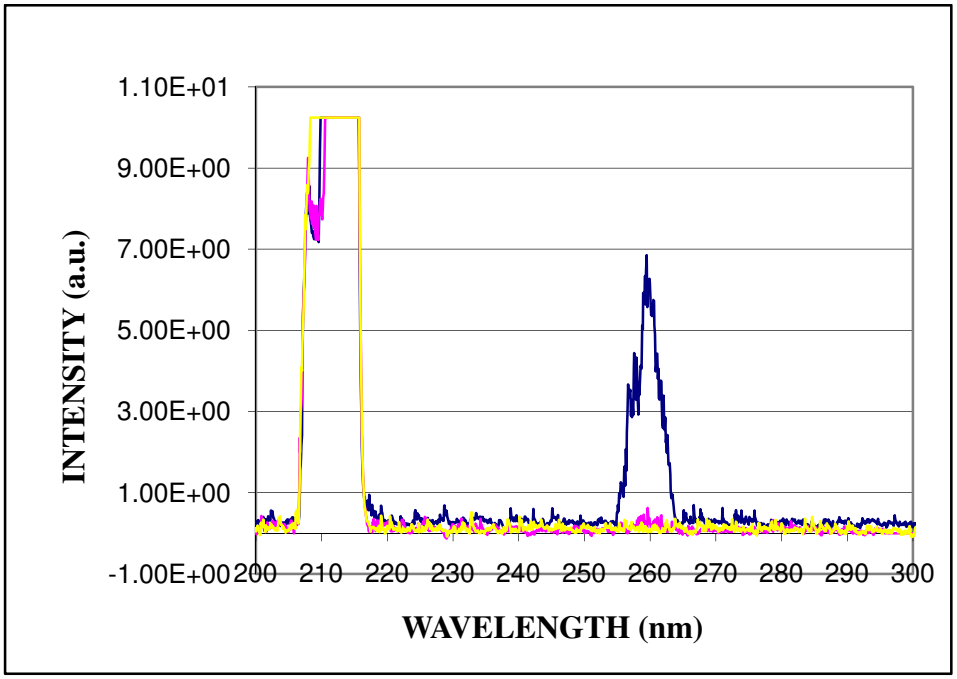


*Figure 18. Sb fluorescence emission scans*

Shown in Figure 18 are three fluorescence spectra. The upper spectrum corresponds to a 10 ppb solution of Sb. The lower two spectra correspond to a blank solution (no antimony) and the other to the removal of the HG reagents (water only). As the spectra show, a very low signal was observed when Sb was not present which demonstrates the high signal to background ratio achieved with the LIF approach.

### 5.1.2. POWER DEPENDENCE CURVE:

At low source intensity, fluorescence emission is proportional to the intensity of the light source. At higher intensity, the fluorescence emission becomes independent of the source intensity. A plot of the fluorescence intensity as a function of laser energy is known as a power dependence curve. Shown in Figure 19 is a power dependence curve for antimony. From the plot, it is seen that as the laser energy increases, the fluorescence intensity also increases almost linearly and then tends towards a limiting value after which it increases only very slowly. This indicated that the fluorescence signal was nearly saturated and would not increase significantly with any more light coming from the laser. This is important because the curve indicates that the largest fluorescence signals are obtained when the laser energy is high. It also indicates that when the laser energy is sufficiently high (approximately 3-4 μJ), the signal becomes nearly independent of changes or variations in the laser energy. This effectively minimizes laser variation as a source of noise in these measurements.

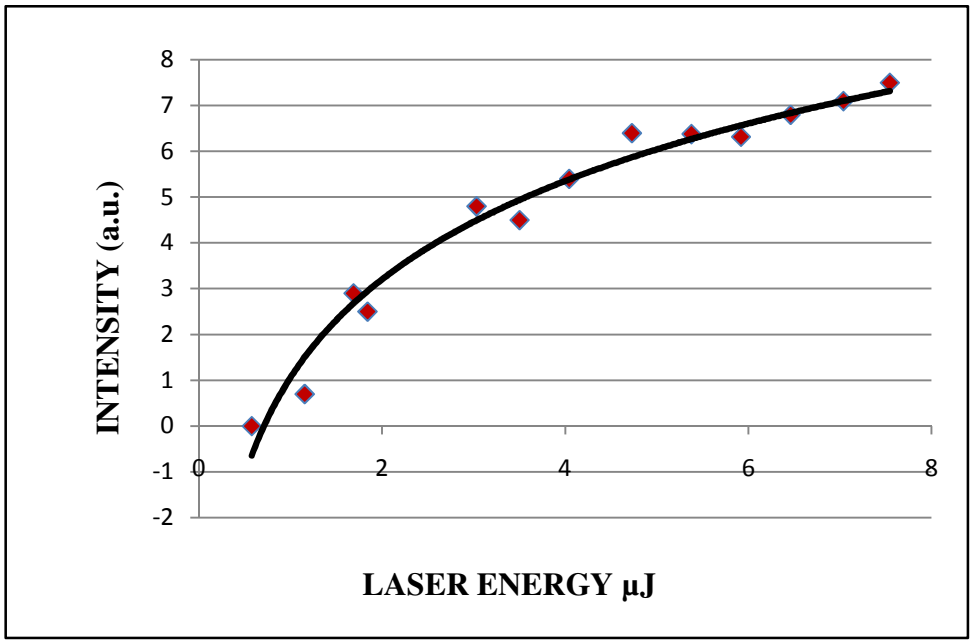


*Figure 19. Power Dependence Curve for Sb*

### 5.1.3. OPTIMIZATION OF LIF USING DIFFERENT CONCENTRATIONS OF HYDROCHLORIC ACID (HCl) AND SODIUM BOROHYDRIDE ($NaBH_4$):

In order to perform calibration curves, the HG-LIF system was optimized using different concentrations of hydrochloric acid (HCl) and sodium borohydride ($NaBH_4$) used as HG reagents. Studies of the signal dependence on the concentrations of HCl and $NaBH_4$ were performed using standard solutions containing 1 and 3 ppb antimony. Plots of the measurements performed using different concentrations of HCl and $NaBH_4$ are shown in Figure 20 and Figure 21, respectively.

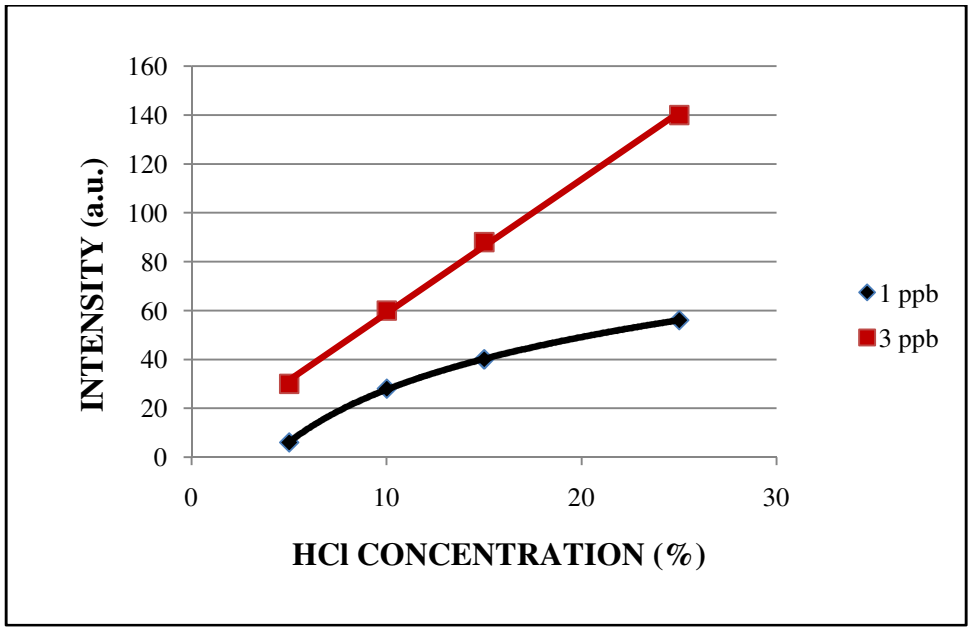


*Figure 20. Concentration of HCl vs. Fluorescence Intensity*

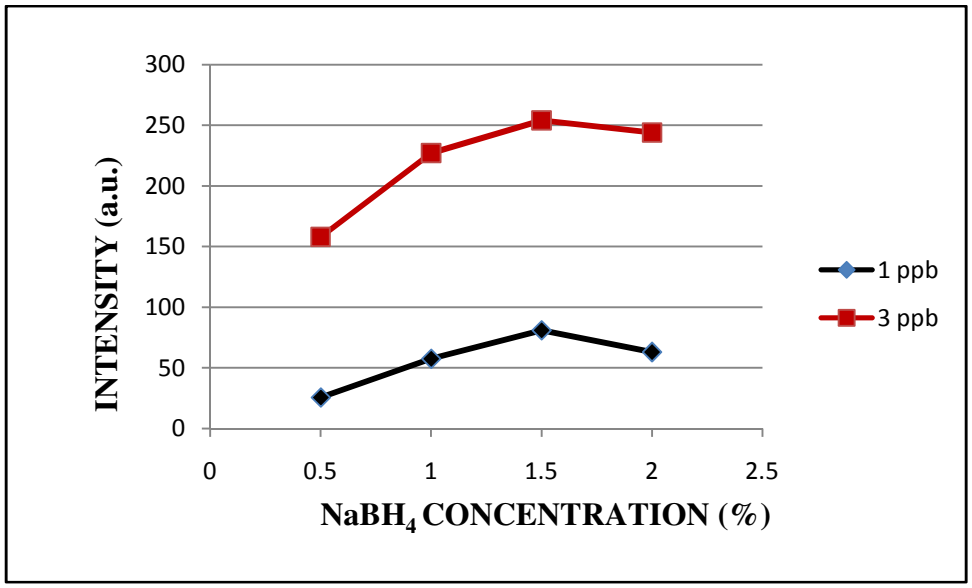


*Figure 21. Concentration of $NaBH_4$ vs. Fluorescence Intensity*

From the plots, it is observed that as the concentration of HCl increases, the fluorescence intensity also increases linearly. In the case of $NaBH_4$, the fluorescence intensity

increases up to certain point and then reaches a maximum point after which it decreases. Although the highest concentrations of HCl produced strong signals, it was decided to use concentrations of HCl and $NaBH_4$ of 10% and 1.5%. These conditions are similar to those reported previously for HG-LIF studies of Sb.[21]

### 5.1.4. CALIBRATION CURVES:

Calibration curves of the fluorescence response of Sb were obtained using different concentrations of antimony (0.1, 0.3, 1, 3, and 10 ppb). According to the fluorescence principle, the fluorescence intensity should be linearly proportional to the concentration of Sb. Initial calibration curves obtained did not show a linear response. It was observed that the fluorescence intensity increased linearly at lower concentrations, but as the concentration of Sb increased further, the intensity tended to reach a saturation point and did not show further increases. This suggested that the detector might not be able to respond linearly at high light levels. Preliminary studies gave a calibration curve as shown in Figure 22.

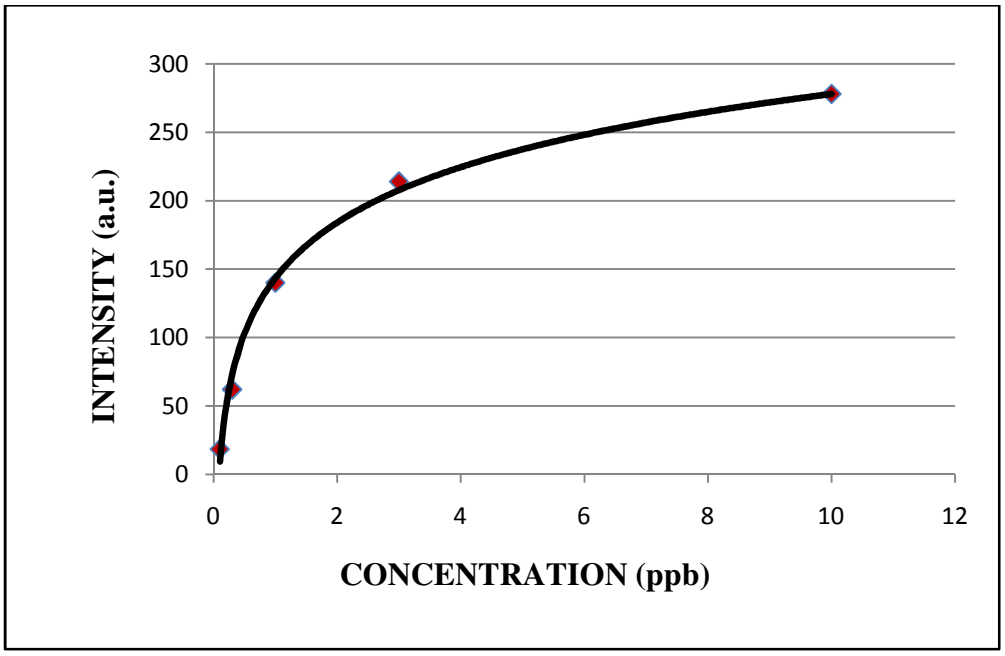


***Figure 22. Calibration curve Sb-HG-LIF without ND filters***

As the calibration curve obtained above was not as expected, Neutral Density (ND) filters were used to attenuate the fluorescence emissions at higher concentrations. For example, a ND 1 filter allows only 10% of light to reach the detector. Calibration curves obtained using ND filters were linear indicating that the fluorescence intensity was linearly proportional to the concentration of the analyte. Calibration curves obtained when ND filters were used as needed at higher concentration are shown in Figure 23 and Figure 24.

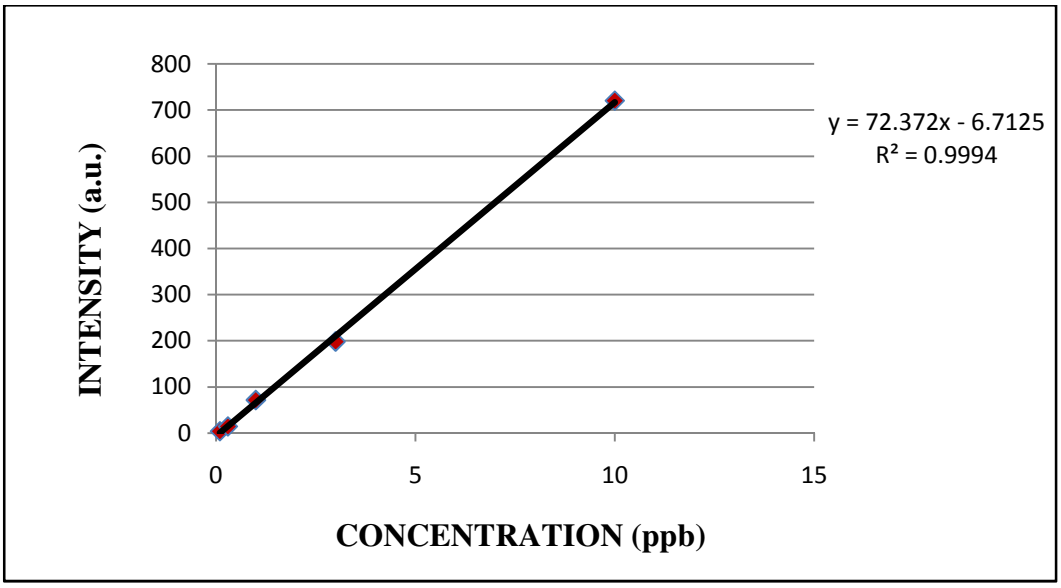


*Figure 23. Calibration curve using ND filters*

Calibration curves were repeated several times to obtain the best limit of detection (LOD) and slope.

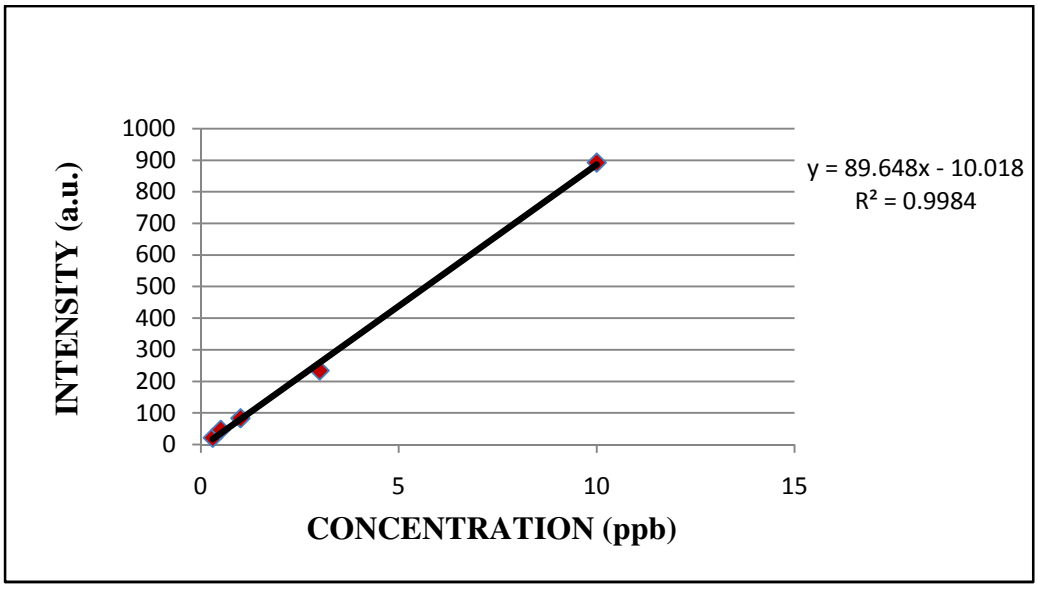


*Figure 24. Calibration curve for Sb using the Sb-HG-LIF technique*

Once a calibration curve is obtained, the slope is determined from the curve and the LOD can be calculated. The limiting noise was estimated by 16 measurements of a blank solution. The standard deviation obtained during the above calibration curve was 0.093274 and the LOD obtained from the LIF studies was 0.003 ppb. Limits of detection obtained from these studies are comparable to previous reports of Sb determination by HG approaches, including HG-LIF.[21]

### 5.1.5. CONDITIONS EMPLOYED IN THE MEASUREMENT OF ANTIMONY USING THE LIF APPROACH:

The following conditions were employed during the measurement of antimony by the LIF technique:

| CONDITIONS | LIF (Sb) |
|---|---|
| Concentrations of metal solutions | 0.3, 0.5, 1, 3, 5 and 10 ppb |
| Absorption wavelength | 212.739 nm |
| Emission wavelength | 259.805 nm |
| PMT voltage | -1200 V |
| Monochromator Slit Width | 1500 µm |
| Time Delay ($t_d$) | - |
| Time Width ($t_w$) | - |
| Averaging | 256 |

***Table 2. Conditions employed for detection of Sb by LIF technique***

### 5.1.6. DISCUSSION:

High sensitivities were observed for antimony measurements using continuous flow HG with LIF detection. The limit of detection obtained by using HG-LIF was in the pptr range and was low when compared to other detection techniques employed for the measurement of antimony as shown in Table 3.

| METHOD | LOD Sb (ppb) | REFERENCES |
|---|---|---|
| HG-AAS | 0.01 | Apte *etal;* 1986[64] |
| HG-AFS | 0.007 | El-Hadri *etal;* 2000[65] |
| ICP-MS | 0.02 | Yang *etal;* 2002[66] |
| HG-ICP-AES | 0.2 | Sayago *etal;* 2000[60] |
| HG-LIF | 0.0003 | Pacquette *etal;* 2001[21] |
| HG-LIF | 0.003 | This work |
| HG-LIBS | 1570 | This work |

***Table 3. Comparison of HG-LIF technique with other techniques***

It is worth noting that the LIF technique also has a high spectral selectivity and will not be affected by the same interferences that can affect atomic absorption spectrometry (AAS) and ICP-MS measurements of these elements. This suggests that it may be better suited for measurements of Sb in complex samples.

## 5.2. INDUCTIVELY COUPLED PLASMA ATOMIC EMISSION SPECTROSCOPY (ICP-AES) STUDIES:

### 5.2.1. HYDRIDE GENERATION COUPLED TO INDUCTIVELY COUPLED PLASMA ATOMIC EMISSION SPECTROSCOPY (HG-ICP-AES):

In this study, the analytical performance of a hydride generation-ICP-AES approach for measurements of antimony and selenium was evaluated.

#### 5.2.1.1. Sb-HG-ICP-AES:

Initial HG-ICP-AES efforts included locating the emission line for antimony. The lines located for antimony were 187.081 nm, 206.813 nm and 217.575 nm. A method was developed for performing a calibration curve for antimony for each located line. Sixteen blanks were measured to determine the Standard Deviation (σ) and a calibration curve was obtained using different concentrations of antimony (0.03, 0.1, 0.3, 1 and 3 ppm).

***Calibration Curves:***

A calibration curve for Sb at 217.575 nm at different integration time (5, 10 and 20 seconds) is shown in Figure 25. Online hydride generation was performed using 10% HCl and 1.5% $NaBH_4$.

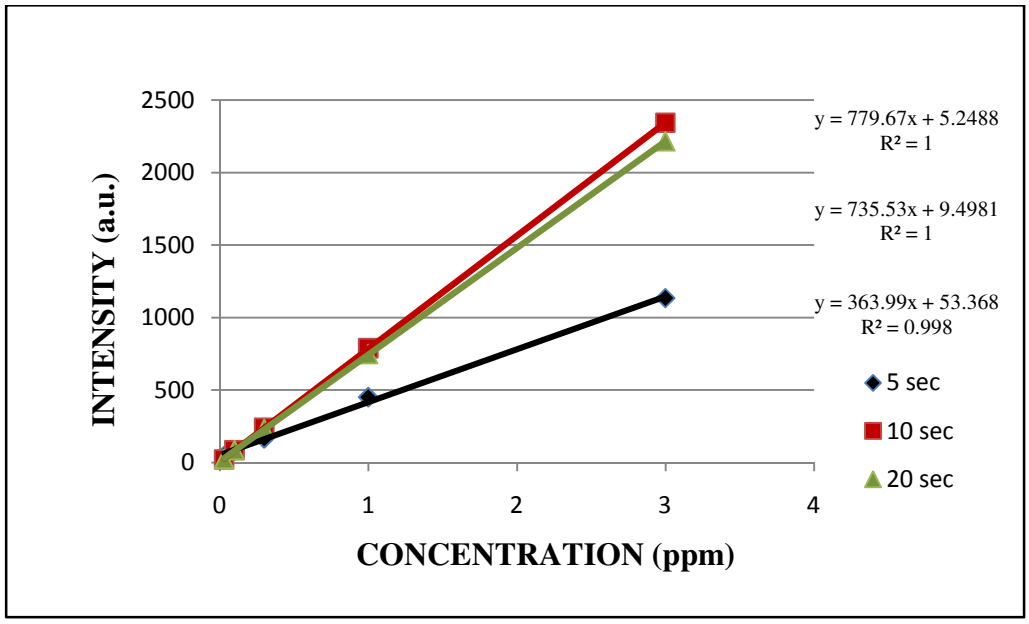


***Figure 25. Calibration Sb-HG-ICP-AES at 217.575 nm using different Integration times***

Limits of detection of 0.16 ppm, 0.018 ppm and 0.02 ppm were obtained when the integration time was adjusted to 5, 10 and 20 seconds, respectively. Keeping the integration time constant at 5 seconds, the located line wavelength for antimony was changed and calibration curves were performed. Wavelengths of 187.081 nm and 206.813 nm were used for the determination of Sb by HG-ICP-AES.

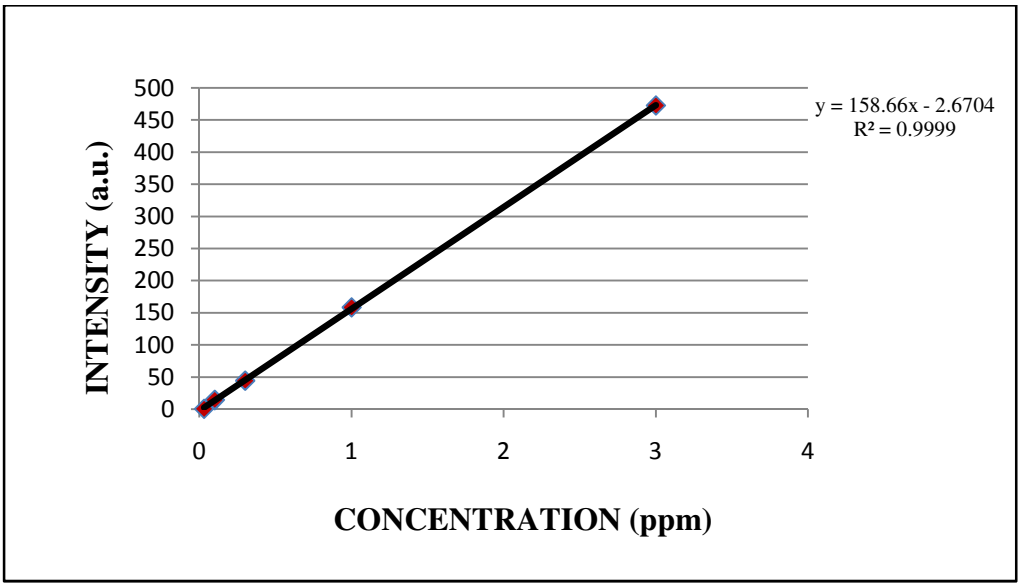


*Figure 26. Calibration Sb-HG-ICP-AES at 187.081 nm*

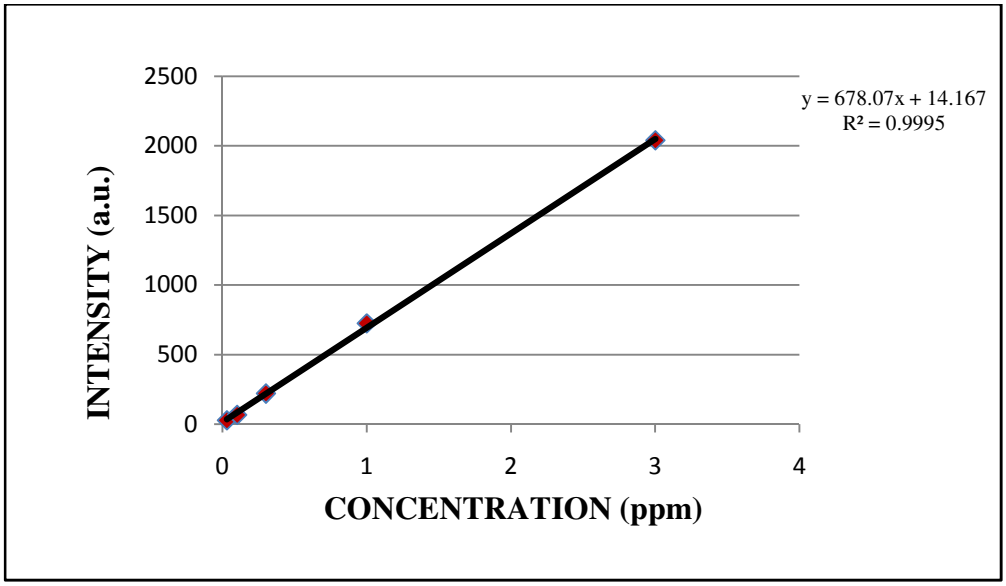


*Figure 27. Calibration Sb-HG-ICP-AES at 206.813 nm*

Limits of detection of 0.07 ppm and 0.03 ppm were obtained at 187.081 nm and 206.813 nm, respectively. The limits of detection obtained from these studies are high compared to previous reports of HG-ICP-AES determination of Sb.[58] Since HG is

expected to provide enhanced sensitivity compared to ICP-AES without HG, the lower sensitivity here may indicate inefficient transfer of the hydride to the ICP torch.

### 5.2.1.2. Se-HG-ICP-AES:

Like antimony, HG-ICP-AES studies for selenium involved locating the emission wavelength lines. The located lines were found at 203.985 nm and 196.090 nm. A method was developed for performing a calibration curve for selenium for each emission line. Sixteen blanks were measured to determine the Standard Deviation (σ) and a calibration curve was obtained using different concentrations of selenium (0.03, 0.1, 0.3, 1 and 3 ppm).

Calibration curves obtained at 196.090 nm and 203.985 nm with an integration time of 5 seconds are shown in Figure 28 and Figure 29. Selenium hydride was generated using 10% and 1.5% of HCl and $NaBH_4$, respectively.

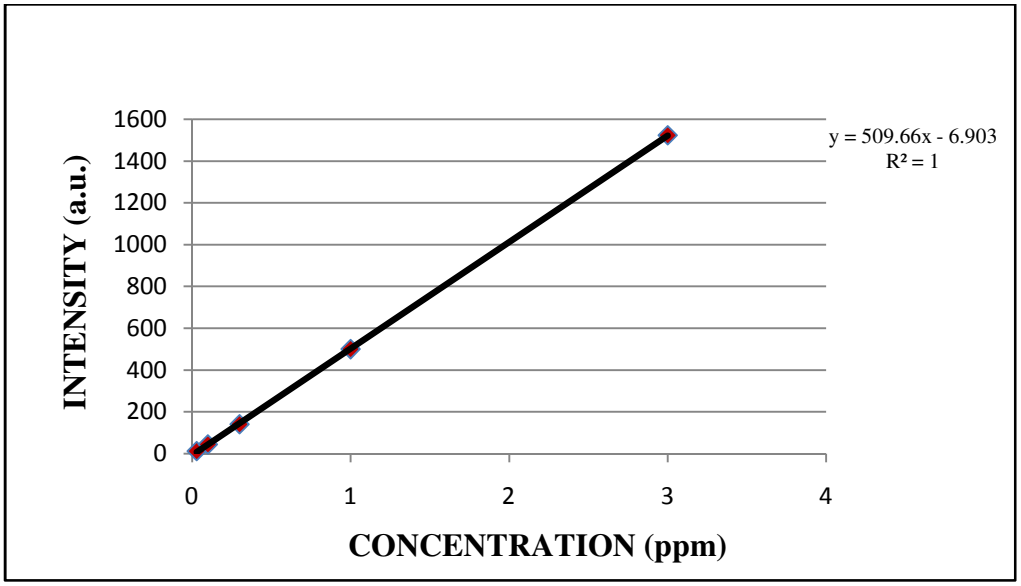


*Figure 28. Calibration Se-HG-ICP-AES at 196.090 nm*

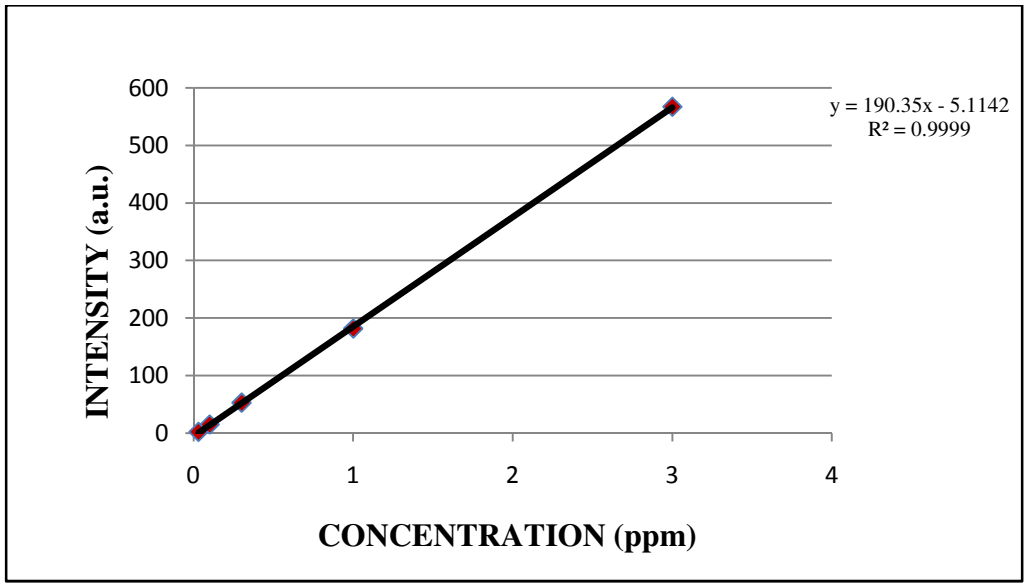


***Figure 29. Calibration Se-HG-ICP-AES at 203.985 nm***

Limits of detection of 0.03 ppm and 0.08 ppm were obtained at wavelengths of 196.090 nm and 203.985 nm, respectively.

### 5.2.2. INDUCTIVELY COUPLED PLASMA ATOMIC EMISSION SPECTROSCOPY (ICP-AES) THROUGH DIRECT NEBULIZATION:

Aluminium, Iron and Manganese were analyzed using the ICP-AES approach. Hydride generation sample introduction was not employed for these elements. The sample was introduced into the instrument by means of a solution nebulizer. An integration time of 5 seconds was used for performing the measurements. For each element, an emission wavelength was located prior to performing a calibration curve. The calibration curves obtained for each of these elements are shown in Figure 30, 31 and 32.

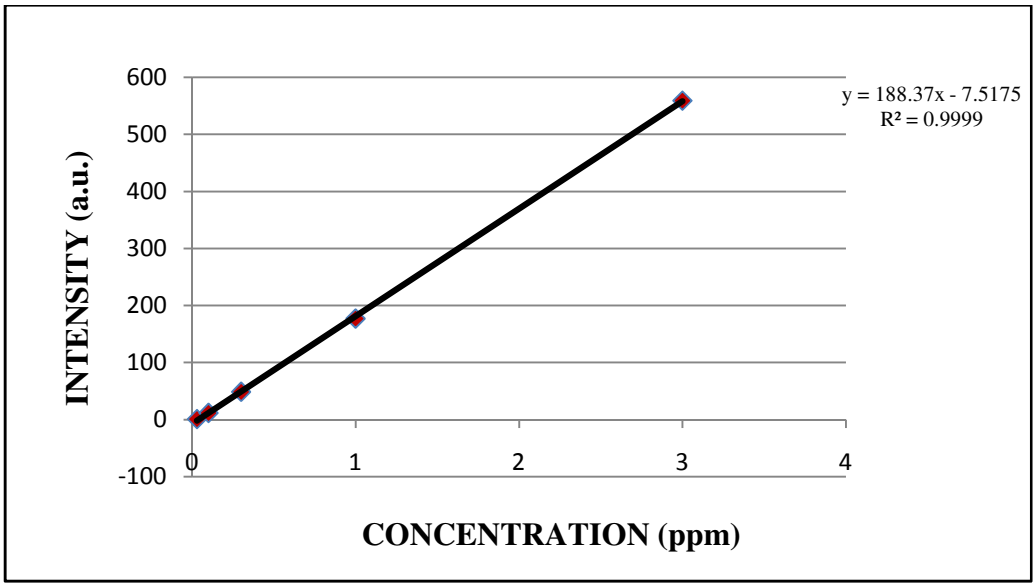


*Figure 30. Calibration Al-ICP-AES at 394.401 nm*

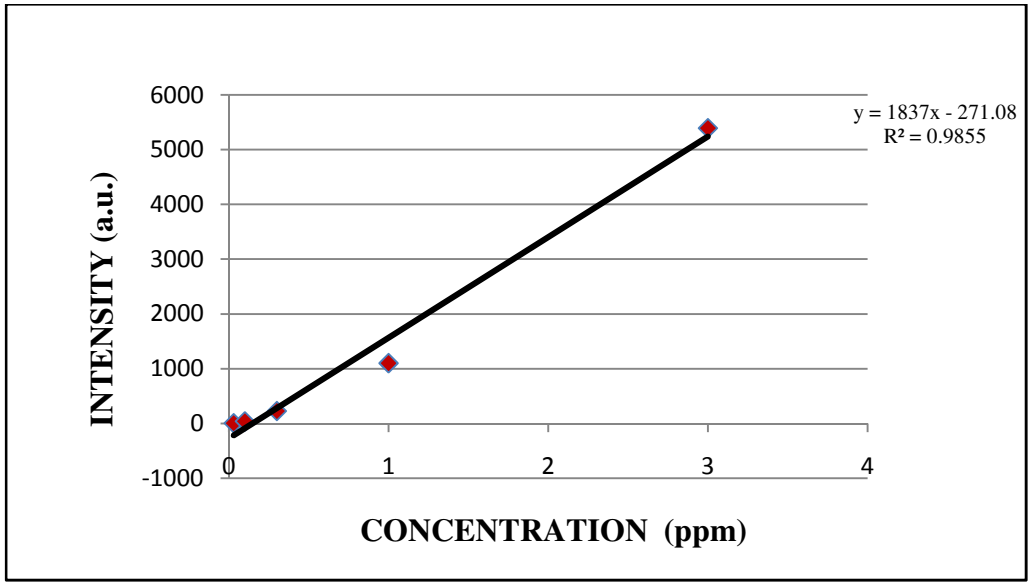


*Figure 31. Calibration Fe-ICP-AES at 273.955 nm*

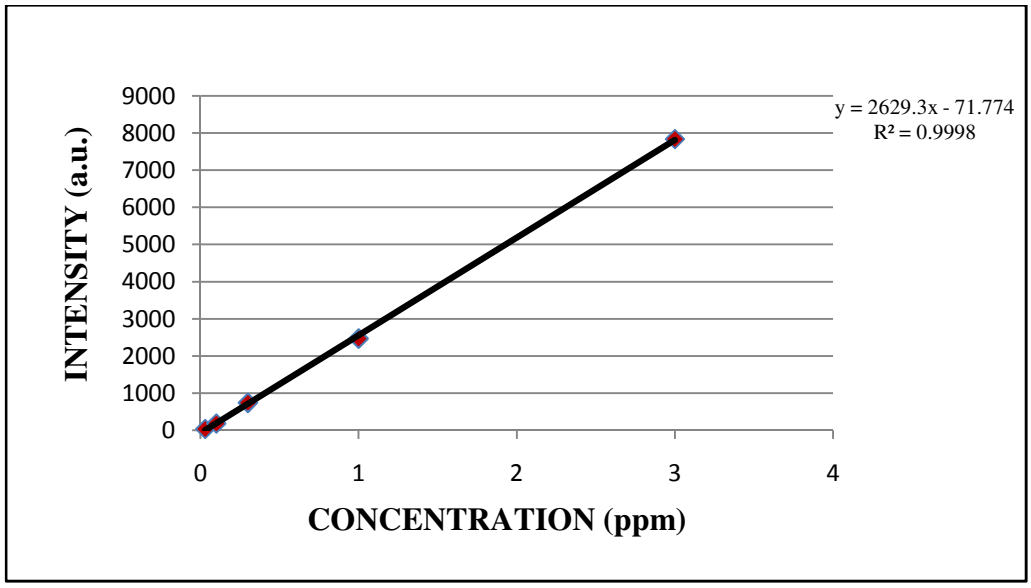


***Figure 32. Calibration Mn-ICP-AES at 293.306 nm***

Limits of detection of 0.03 ppm, 0.01 ppm and 0.009 ppm were obtained for Al, Fe and Mn respectively. The limits of detection obtained for Al, Fe and Mn are high compared to previous reports of determination of these elements by ICP-AES.[42, 59]

### 5.2.3. DISCUSSION:

Hydride generation coupled directly to the ICP-AES spectrometer provided LODs in the ppb range. It was found that the sensitivity of this approach was good but it was anticipated that HG sample introduction might lead to even better sensitivity due to better sample efficiency. Further experiments to improve the sensitivity could not be carried out as there was a problem with the instrument due to which the instrument could not be used any further.

## 5.3. LASER INDUCED BREAKDOWN SPECTROSCOPY (LIBS) STUDIES:

Following studies using the ICP instrument, further emission studies were performed using an alternate plasma source, specifically a laser produced plasma. The analytical capability of a method using HG sample introduction and LIBS detection was evaluated for antimony and selenium.

### 5.3.1. STUDIES USING A 355 nm LASER:

#### 5.3.1.1. Sb-HG-LIBS:

An emission spectrum of antimony using the LIBS technique indicated that a strong emission wavelength of antimony was at 259.805 nm. A spectrum of antimony showing emission near 259.8 nm is shown in Figure 33. The monochromator slit width was adjusted to 50 µm, the averaging was adjusted to 30, and the signal sensitivity was set at 10 mV/V. Different delays and widths were adjusted on the boxcar to obtain the best signal to noise. The optimum signal was obtained when the delay ($t_d$) and width ($t_w$) were 1 µs and 3 µs, respectively, on the boxcar.

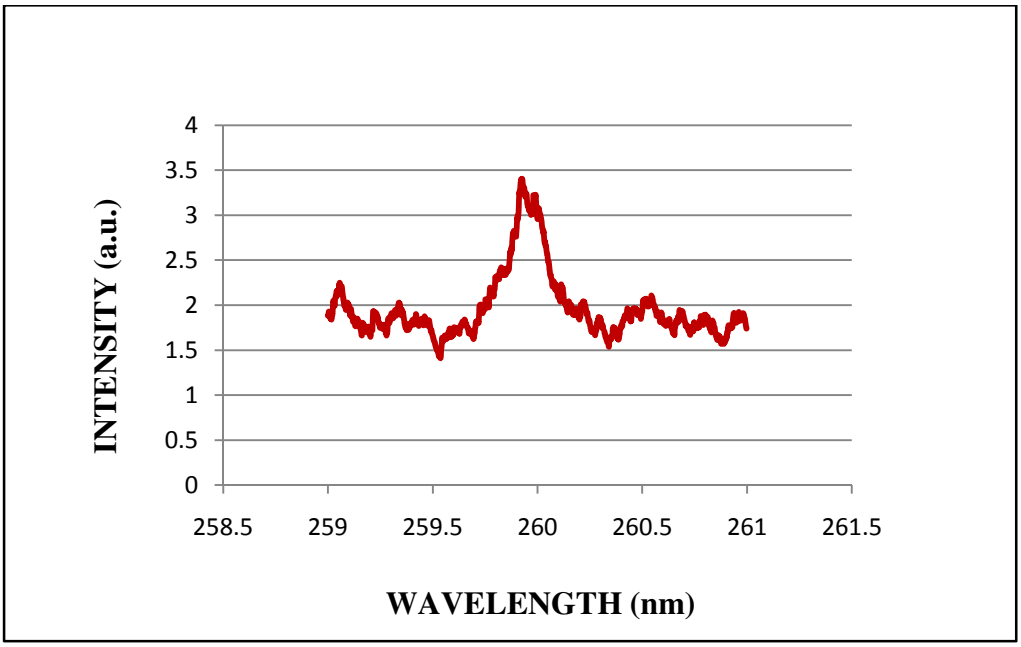


***Figure 33. Emission spectrum of Sb at 259.8 nm using LIBS***

To obtain the maximum point of emission, intensities were measured at 259.8 nm, 259.9 nm and 260 nm using a 10 ppm solution of Sb as indicated in Table 4. From the table, it is seen that the maximum intensity was observed at a wavelength of 259.9 nm.

| **Wavelength (nm)** | **$t_d$ (µs)** | **$t_w$ (µs)** | **Avg** | **Slit width (µm)** | **Signal (mV/V)** | **$NaBH_4$, HCl (%)** | **PMT (V)** | **Flow rates of Ar (sccm)** | **Scan rate (nm/min)** | **Max intensity** |
|---|---|---|---|---|---|---|---|---|---|---|
| 259.8 | 1 | 1 | 30 | 50 | 10 | 1.5, 10 | -1200 | 40, 40 | 1 | 0.814 |
| 259.9 | 1 | 1 | 30 | 50 | 10 | 1.5, 10 | -1200 | 40, 40 | 1 | 1.054 |
| 260 | 1 | 1 | 30 | 50 | 10 | 1.5, 10 | -1200 | 40, 40 | 1 | 0.242 |

***Table 4. Parameters used in the LIBS technique for detection of Sb***

Calibration curves were performed using different slit widths (50, 100 and 150 µm) on the monochromators. Different concentrations of antimony solutions (1, 2, 3, 5, 7 and 10 ppm) were used. The series of calibration curves is shown in Figure 34.

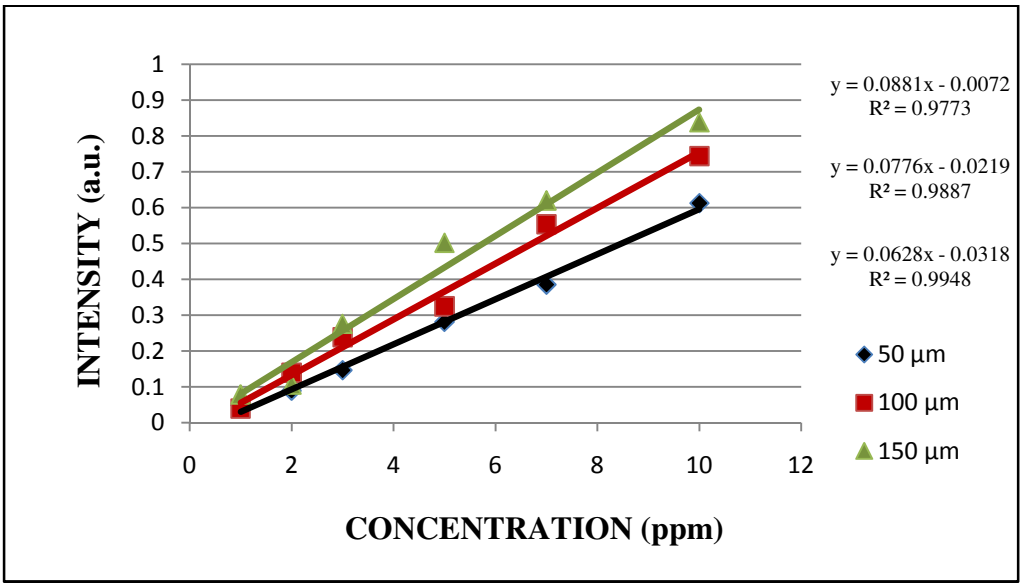


***Figure 34. Calibration Sb-HG-LIBS using different slit widths***

A limit of detection of 1.6 ppm was obtained when the calibration curve was performed using a monochromator slit width of 50 µm.

**5.3.1.1.1. INTERFERENCES INVOLVED IN THE MEASUREMENT OF ANTIMONY:**

It has been reported that some elements can cause interferences in HG measurements of metals and metalloids.[60] To observe the possible effect of selenium on antimony, a 10 ppm solution of Se was added to each concentration of Sb solution that was used in obtaining a calibration curve for antimony (Figure 35).

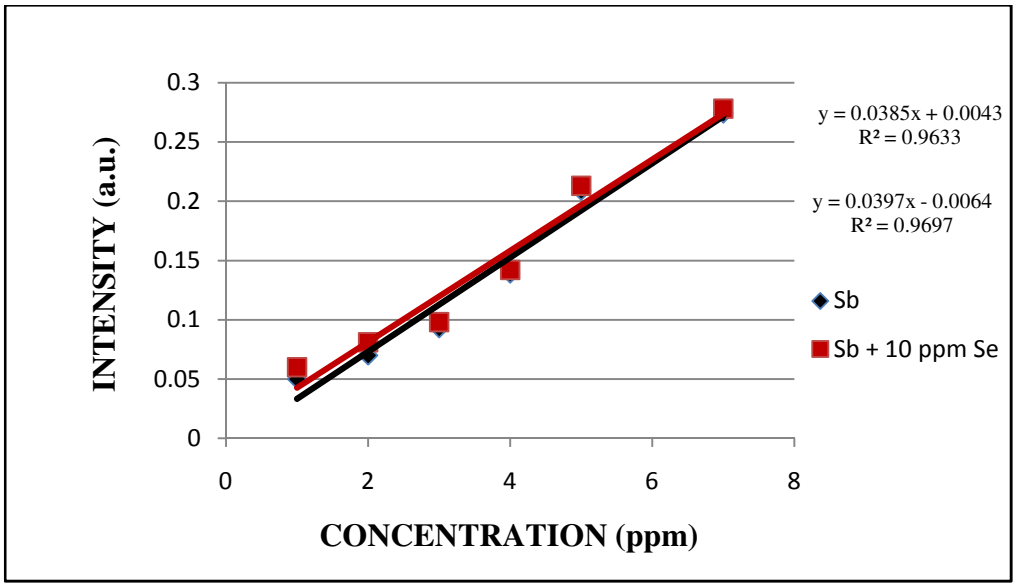


***Figure 35. Effect of Se on the measurement of Sb***

From the above plot, it is observed that Se has no apparent effect on the measurement of Sb. Thus Sb can be analyzed in the presence of Se at this level with no measurement interferences. This result agrees with previous reports of interferences in HG approaches.[60]

**5.3.1.1.2. SPECIATION OF ANTIMONY:**

It has been reported that selective hydride generation for Sb can be performed by using different solution pH values.[17, 55] At low pH, both Sb(III) and Sb(V) are expected to give a response while at pH 6-7, only Sb(III) is expected to give a signal. Although this approach was tested, it was not successfully demonstrated and is still under development.

### 5.3.1.2. Se-HG-LIBS:

An emission spectrum of selenium using the LIBS technique indicated that the emission wavelength of selenium was at 196.1 nm. Prior to obtaining the calibration curve of selenium, the parameters on the boxcar ($t_d$ and $t_w$) were adjusted to give the best emission spectrum. The spectra of selenium at different delays (500 ns, 700 ns and 1 µs) and width (1.5 µs, 2 µs and 3 µs) are shown in Figure 36 and 37, respectively.

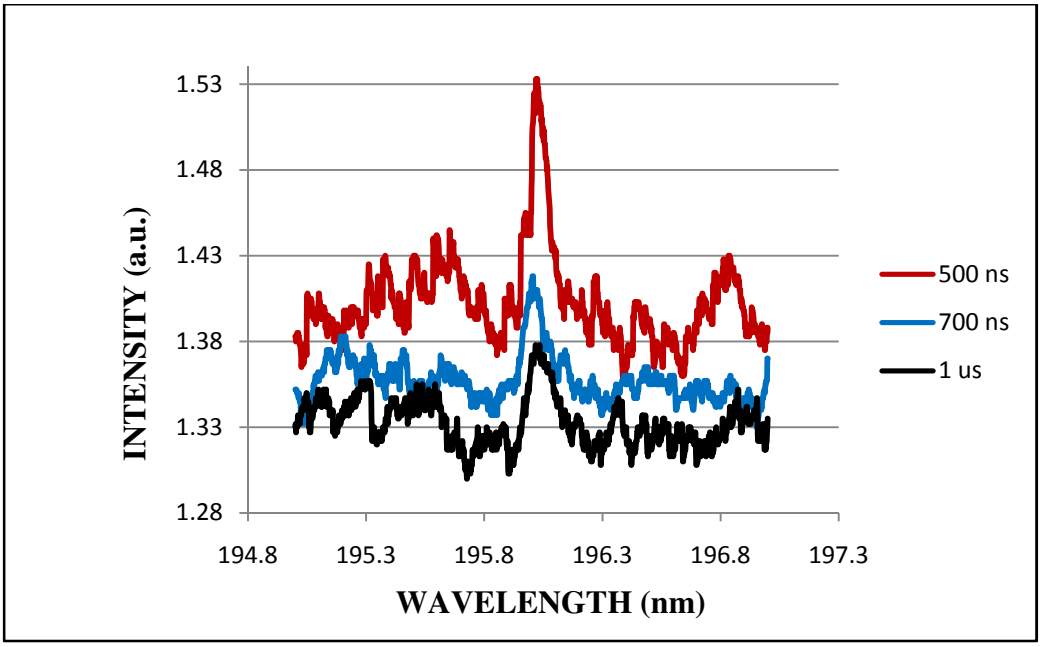


***Figure 36. Spectrum of Se at different delays***

Different delays ($t_d$) on the boxcar allowed adjustment of the measurement time from when the laser plasma begins until the time the emission decays. By adjusting the delays on the boxcar, the intensity of the plasma emission at different times can be measured.

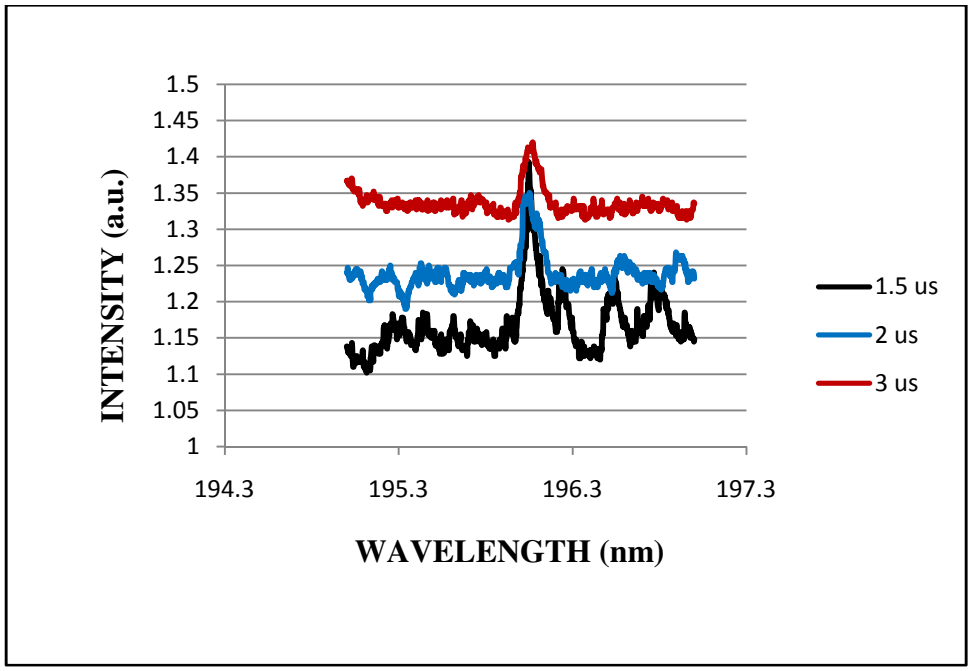


***Figure 37. Spectrum of Se at different widths***

Changing the widths ($t_w$) in the boxcar gate allowed adjustment of the time over which the plasma light is measured. By adjusting the widths on the boxcar, the intensity of the plasma providing the maximum signal to background ratio can be selected. For measurement of Se using the LIBS technique, it was observed that a width of 1.5 µs gave a peak with maximum intensity, that of 2 µs produced a peak of intermediate intensity while that of 3 µs produced a peak of lower intensity. It should be noted that the best measurements did not necessarily correspond to times when the signal intensities were stronges.

It was observed that the best results were obtained when the $t_d$ and $t_w$ were adjusted to 700 ns and 3 µs respectively. A spectrum of selenium with these parameters is shown in Figure 38.

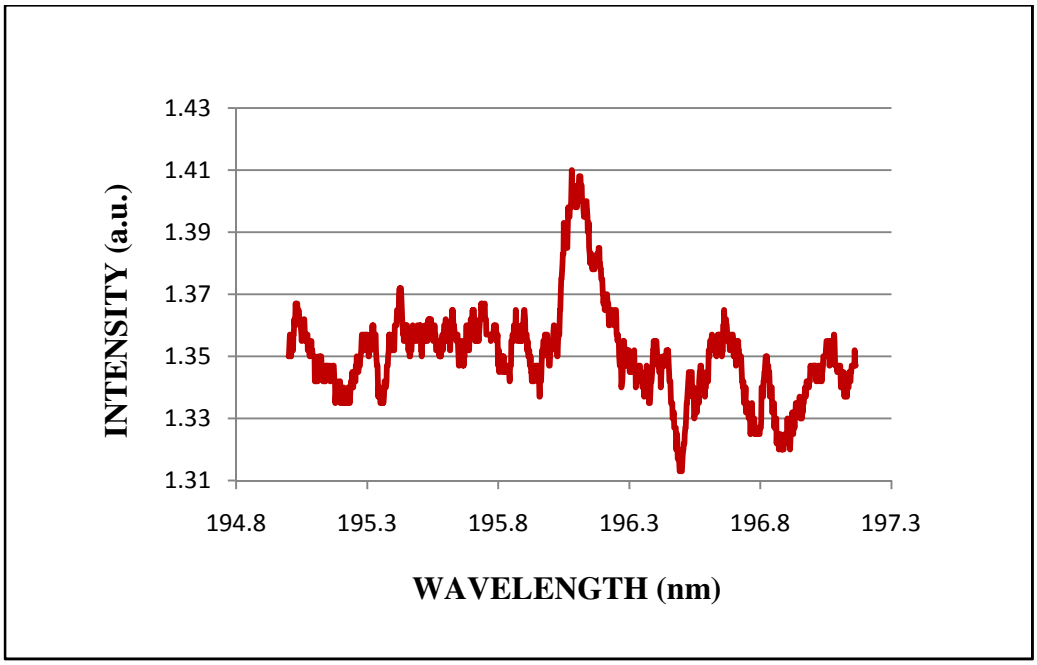


*Figure 38. Emission Spectra of Se at 196.1 nm*

| **Wavelength (nm)** | **$t_d$ (ns)** | **$t_w$ (µs)** | **Avg** | **Slit width (µm)** | **Signal (mV/V)** | **$NaBH_4$, HCl (%)** | **PMT (V)** | **Flow rates of Ar (sccm)** | **Scan rate (nm/min)** | **Max intensity** |
|---|---|---|---|---|---|---|---|---|---|---|
| 196.0 | 700 | 3 | 30 | 20 | 10 | 1.5, 10 | -1200 | 40, 40 | 1 | 1.274 |
| 196.1 | 700 | 3 | 30 | 20 | 10 | 1.5, 10 | -1200 | 40, 40 | 1 | 1.419 |
| 196.2 | 700 | 3 | 30 | 20 | 10 | 1.5, 10 | -1200 | 40, 40 | 1 | 1.302 |
| 196.3 | 700 | 3 | 30 | 20 | 10 | 1.5, 10 | -1200 | 40, 40 | 1 | 1.290 |

*Table 5. Parameters used in the LIBS technique for detection of Se*

To obtain the maximum point of emission, intensities were measured at 196.0 nm, 196.1 nm, 196.2 nm and 196.3 nm using a 10 ppm solution of Se as indicated in Table 5.

From the table, it can be seen that the maximum intensity is observed at a wavelength of 196.1 nm.

Calibration curves at 196.1 nm were obtained by using different monochromator slit widths (10, 30, 50, and 100 µm). Different concentrations of selenium solutions (1, 2, 3, 5, 7 and 10 ppm) were used to obtain the calibration curves that are shown below in Figure 39.

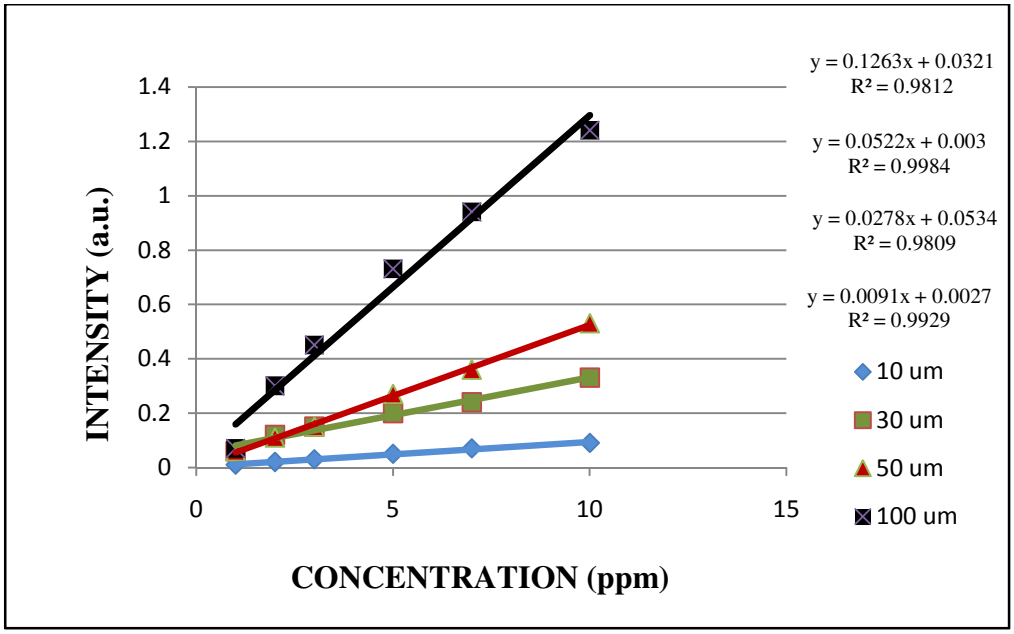


***Figure 39. Calibraton Se-HG-LIBS at 196.1 nm using different slit widths***

As expected, increasing the slit width increases the amount of light reaching the detector resulting in higher responses and a higher slope for the calibration curve. A limit of detection of 0.97 ppm was obtained when the monochromator slit width was adjusted to 50 µm. LIBS measurements have been performed in the past for arsenic and other metals and limits of detection obtained were also in the ppm range.[70] Thus the results obtained from this study compare well with previous studies.

### 5.3.1.2.1. INTERFERENCES INVOLVED IN THE MEASUREMENT OF SELENIUM:

The effects of Tin (Sn) and Antimony (Sb) on the measurement of Se by HG-LIBS were evaluated. To observe the effect of Sb on Se, a 10 ppm solution of Sb was added to each concentration of Se solution that was used in obtaining a calibration curve. A plot of the results of HG-LIBS measurements of these solutions is shown in Figure 40.

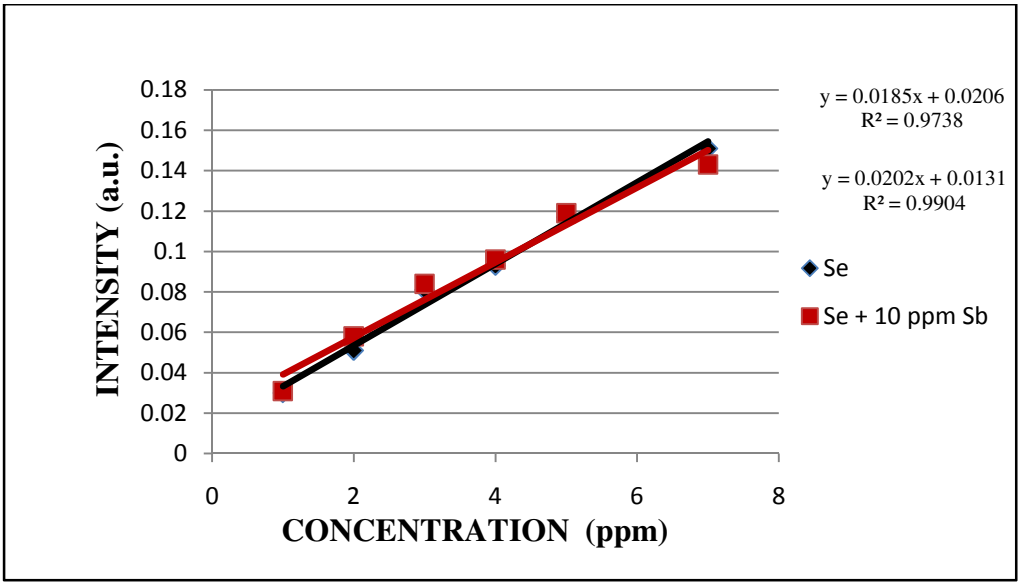


***Figure 40. Effect of Sb on the measurement of Se***

From the above plot, it is seen that Sb has no apparent effect on the measurement of Se. Thus Se can be analyzed in the presence of Sb at these concentrations with minimal interferences. These results are consistent with previous studies of these interferences.[61]

Likewise, the effect of Sn on Se was evaluated. A 10 ppm solution of Sn was added to each concentration of Se solution that was used in obtaining a calibration curve. The plot of the results of these measurements is shown in Figure 41. From the graph, it

can be observed that Sn may cause a negative interference in the measurement of Se by HG-LIBS at these concentrations.

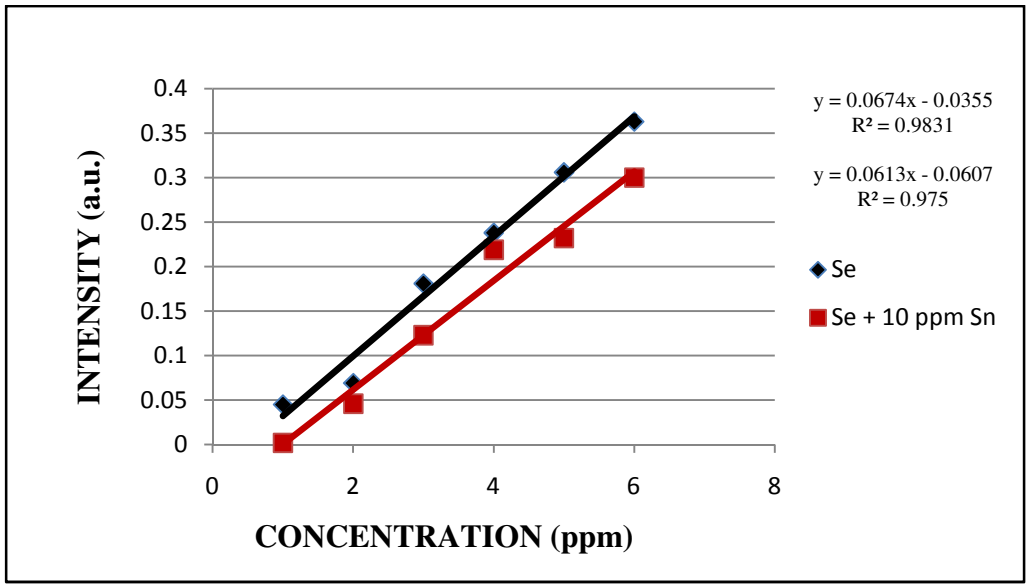


***Figure 41. Effect of Sn on the measurement of Se***

**5.3.1.2.2. SPECIATION OF SELENIUM:**

Due to the importance of Se speciation, an approach has been investigated for spectiation measurements of Se. Speciation for Se has been accomplished using a pre-reduction procedure for selenate.[62] Under normal HG conditions, only selenite gives a response. However, when the sample is acidified and boiled for 15-20 min with 4 M HCl,[63] the selenate species are reduced to selenite and are able to be measured by HG-LIBS. In this way, the two species can be determined selectively by different sample treatment procedures. The parameters used for the speciation measurements are shown in Table 6.

| $t_d$ (ns) | $t_w$ (µs) | Avg | Signal (mV/V) | $NaBH_4$, HCl (%) | PMT (V) | Scan rate (nm/min) |
|---|---|---|---|---|---|---|
| 700 | 3 | 1000 | 10 | 1.5, 10 | -1200 | 1 |

***Table 6. Parameters used for the speciation of Se by LIBS***

The speciation responses for selenite and selenate are reported in Table 7.

| SAMPLE | Before Acidification of Standard Solutions | After Acidification of Standard Solutions |
|---|---|---|
| | 50 µm slit width | 50 µm slit width |
| Selenite | 0.119 | 0.117 |
| Selenate | 0.007 | 0.137 |

***Table 7. Responses obtained during the speciation of Se by LIBS***

As the results show, selenite and selenate produce significantly different responses by the two sample preparation procedures indicating that speciation can be performed.

### 5.3.1.3. CONDITIONS EMPLOYED IN THE MEASUREMENT OF ANTIMONY AND SELENIUM USING THE LIBS APPROACH:

The following conditions were employed during the measurement of antimony and selenium by the LIBS technique:

| CONDITIONS | LIBS (Sb) | LIBS (Se) |
|---|---|---|
| Concentrations of metal solutions | 1, 2, 3, 5, 7 and 10 ppm | 1, 2, 3, 5, 7 and 10 ppm |
| Absorption wavelength | - | - |
| Emission wavelength | 259.8 nm | 196.1 nm |
| PMT voltage | -1200 V | -1200 V |
| Monochromator Slit Width | 50 µm | 100 µm |
| Time Delay ($t_d$) | 1 µs | 700 ns |
| Time Width ($t_w$) | 3 µs | 3 µs |
| Averaging | 1000 | 1000 |

***Table 8. Conditions employed in the measurement of Sb and Se by LIBS***

### 5.3.2. STUDIES USING A 532 nm LASER:

Due to intermittent problems with the laser at 355 nm, the laser was changed to operate at 532 nm for HG-LIBS measurements. This higher energy laser source was used for further studies of antimony and selenium by HG-LIBS.

#### 5.3.2.1. Se-HG-LIBS:

Preliminary studies using the 532 nm laser were performed for Selenium. When the monochromator slit width was adjusted to 10 µm, no filters were required to attenuate the plasma emission. However, a 20 µm slit width required a 0.4 ND filter and slit widths

of 50 µm and 100 µm required a 1 ND filter each. To determine the best parameters on the boxcar, different delays (500 ns, 700 ns, 1 µs, 2 µs and 3 µs) and a width of 3 µs were used to obtain the spectrum of selenium emission near 196.1 nm. A slit width of 20 µm with 0.4 ND filter was used to obtain the spectrum. The best spectrum was obtained when $t_d$ was 1 µs and the $t_w$ was adjusted to 3 µs. The maximum wavelength of emission using this laser was found to be 196.1 nm. This spectrum is shown in Figure 42.

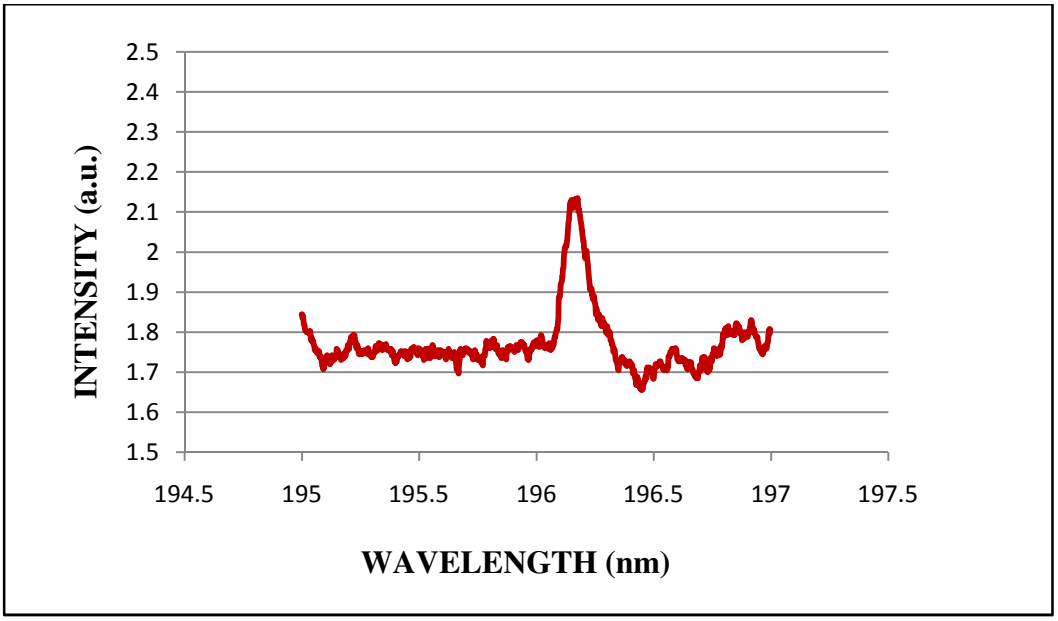


***Figure 42. Emission Spectra of Se at 196.1 nm***

Setting the monochromator at 196.1 nm, calibration curves were obtained for different concentrations of Se (1, 2, 3, 5, 7 and 10 ppm). Different slit widths were used and ND filters were used for higher slit widths when a large plasma volume was viewed by the detector. A calibration curve of Se with different slit widths is shown in Figure 43.

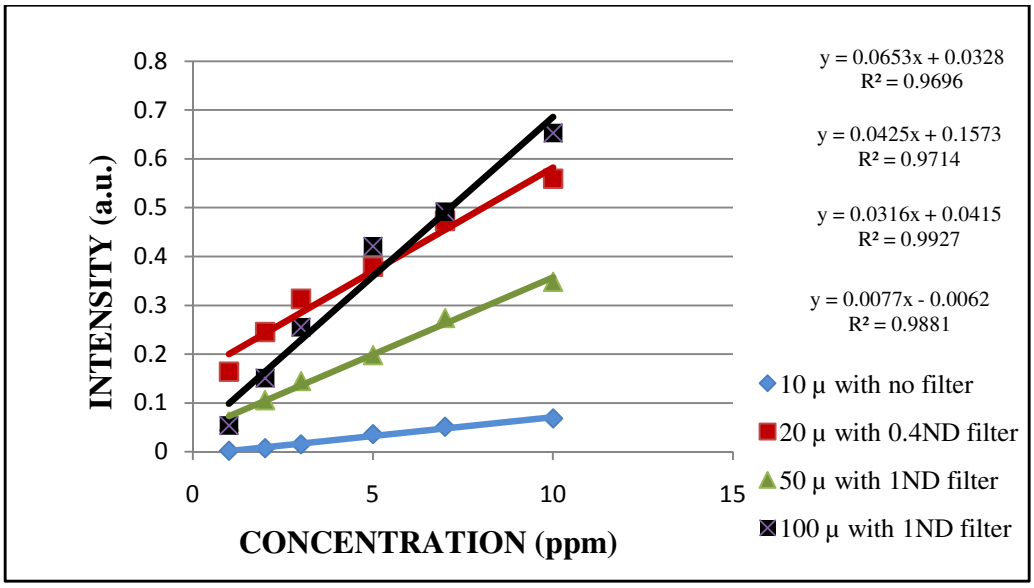


***Figure 43. Calibration Se-HG-LIBS at 196.1 nm using different slit widths***

A limit of detection of 0.02 ppm was obtained when calibration curves were performed using a slit width of 100 µm. This suggests that the use of the higher power 532 nm laser which created more intense plasmas may have contributed to higher sensitivity for Se measurements. This compares favourably to the results obtained using the related HG-ICP-AES approach.

#### 5.3.2.1.1. ETHANOL ENHANCEMENT EFFECT ON SELENIUM:

It has been reported that ethanol can increase the sensitivity of HG approaches for As and Se.[31] In this study, the sensitivity was increased by adding ethanol to the solutions of Se. Different solutions with the same concentration (10 ppm) of Se were prepared. The first solution had no ethanol in it, while the rest had increasing percentages of ethanol (1, 2, 3, 4, 5, and 6%). The results obtained showed that the HG-LIBS signal intensity of the ethanol added solution was higher than that without ethanol. This indicates that ethanol

has an enhancement effect on signal intensity. The enhancement effect of ethanol on Se can be observed in Figure 44 which shows that the Se response was increased by 40% when 6% of ethanol is added to the Se solution.

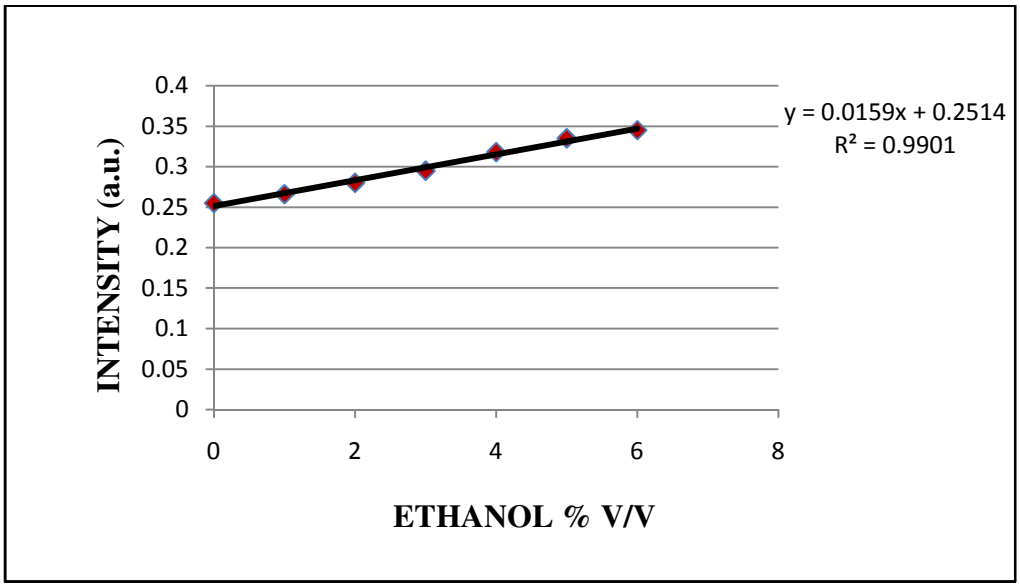


***Figure 44. Ethanol Enhancement Effect on Se***

These results compare well with previous reports of ethanol enhancement effect on Se by HG approaches[31] and suggest that this may be useful for enhancing the sensitivity for other HG approaches.

**5.3.2.2. Sb-HG-LIBS:**

Although Sb was observed previously in these studies by HG-LIBS, Sb did not provide results when measurements were performed with the 532 nm laser. It is possible that the high concentrations of Se, Te, As and Sn solutions used previously may have

caused a memory effect and resulted in a chemical interference that prevented Sb emissions from being observed. This remains to be investigated further.

### 5.3.3. DISCUSSION:

From the limits of detection obtained, it can be said that Laser induced breakdown spectroscopy is a relatively less sensitive technique compared to other HG-based methods. The limits of detection obtained for Sb and Se by the LIBS technique were in the ppm range. A comparison of the limits of detection for Sb and Se obtained by the LIBS technique with other techniques is given in Table 9.

| METHOD | LOD Sb (ppb) | REFERENCES | LOD Se (ppb) | REFERENCES |
|---|---|---|---|---|
| HG-LIF | 0.003 | THIS WORK | 0.00009 | Pacquette *etal;* 2001[21] |
| HG-AFS | 0.007 | El-Hadri *etal;* 2000[65] | 0.003 | Tang *etal;* 2005[71] |
| HG-ICPAES | 0.2 | Sayago *etal;* 2000[60] | 30 | Saisho *etal;* 1990[37] |
| HG-AAS | 0.01 | Apte *etal;* 1986[64] | 0.2 | Zhang *etal;* 2008[72] |
| HG-ICPAES | 30 | THIS WORK | 30 | THIS WORK |
| HG-LIBS | 1600 | THIS WORK | 20 | THIS WORK |

***Table 9. Comparison of HG-LIBS technique with other techniques***

## 5.4. CONCLUSION:

As these studies have shown, a low detection limit has been obtained for Sb with HG-LIF. The LODs obtained using HG-LIF are in the pptr range while the LODs for HG-LIBS are in the ppb to ppm range. Although it is less sensitive than HG-LIF, the HG-LIBS approach still provides trace level sensitivity, is better suited to multi-element analyses and has fewer instrumentation requirements as it only requires one laser. The results also demonstrate that continuous hydride generation is an effective sample introduction method that provides high sensitivities and low detection limits, especially when it is combined with LIF detection. It also has the potential to allow speciation as demonstrated for Se. Compared to other methods, including LIBS, the LIF technique has a high spectral selectivity and is not expected to suffer interferences from species that affect atomic absorption spectrometry (AAS) and ICP-MS measurements.

## 5.5. FUTURE WORKS:

The long term goal of this project is to develop techniques that can be used for sensitive and selective measurements of these elements in different materials. This will include the combination of the HG-LIF and HG-LIBS approaches with chromatographic separation approaches such as HPLC and GC to allow speciation analyses. Further studies of speciation approaches, including the enhancement by additives such as ethanol, should be performed. Further studies of the HG-LIBS should also be performed to improve the sensitivity for Sb, Se and other elements.

# CHAPTER 6: REFERENCES


(1) Thomas J. Manning; William R. Grow Inductively Coupled Plasma-Atomic Emission Spectrometry. *http://www.mrl.ucsb.edu/mrl/centralfacilities/chemistry/icp.pdf*1997).

(2) Robinson, J. W. In *Undergraduate instrumental analysis;* M. Dekker: New York, 1995; , pp 858.

(3) Jones, J. B.; Jr In *Laboratory guide for conducting soil tests and plant analysis;* CRC Press: Boca Raton, Fla., 2001; , pp 363; 333-338.

(4) Juhyoun Kwak Laser-Induced Fluorescence. *http://elchem.kaist.ac.kr/vt/chem-ed/spec/laser/lif.htm*.

(5) Pungor, E. In *A practical guide to instrumental analysis;* CRC Press: Boca Raton, 1995; , pp 384.

(6) Popppiti, J. A. In *Practical techniques for laboratory analysis;* Lewis Publishers: Boca Raton, 1994; , pp 188.

(7) Swarbrick, J.; Boylan, J. C., Eds.; In *Encyclopedia of pharmaceutical technology;* Marcel Dekker: New York, 2002; .

(8) Seiler, H. G.; Sigel, A.; Sigel, H., Eds.; In *Handbook on metals in clinical and analytical chemistry;* M. Dekker: New York, 1994; , pp 753.

(9) Miziolek, A. W.; Palleschi, V.; Schechter, I., Eds.; In *Laser-induced breakdown spectroscopy (LIBS) : fundamentals and applications;* Cambridge University Press: Cambridge, UK ; New York, 2006; , pp 620.

(10) Sneddon, J.; Thiem, T. L.; Lee, Y., Eds.; In *Lasers in analytical atomic spectroscopy;* VCH: New York, 1997; , pp 275.

(11) Castle, B. C. In *Laser-induced breakdown spectroscopy : fundamentals, instrumentation and applications;* 1998; , pp 244.

(12) Cremers, D. A.; Radziemski, L. J., Eds.; In *Handbook of laser-induced breakdown spectroscopy;* John Wiley: Chichester, England ; Hoboken, NJ, 2006; , pp 283 p., [10] p. of.

(13) Lajunen, L. H. J.; Peramaki, P.; Royal Society of Chemistry, Eds.; In *Spectrochemical analysis by atomic absorption and emission;* Royal Society of Chemistry: Cambridge, 2004; , pp 342; 329-331.

(14) Hill, S. J., Ed.; In *Inductively coupled plasma spectrometry and its applications;* Blackwell Pub.: Oxford ; Ames, Iowa, 2007; , pp 427.

(15) Sharaf, M. A.; Illman, D. L.; Kowalski, B. R., Eds.; In *Chemometrics;* Wiley: New York, 1986; , pp 332.

(16) Ulrich, N. *Anal. Chim. Acta*. **1998***, 359*, 245-253.

(17) Andreae, M. O.; Asmode, J. F.; Foster, P.; Van 't dack, Luc *Anal. Chem.* **1981***, 53*, 1766-1771.

(18) Filella, M.; Belzile, N.; Lett, M. *Earth Science Reviews* **2007***, 80*, 195-217.

(19) Cornelis, R.; De Kimpe, J.; Zhang, X. *Spectrochimica Acta Part B: Atomic Spectroscopy* **1998***, 53*, 187-196.

(20) Bohari, Y.; Astruc, A.; Astruc, M.; Cloud, J. *J. Anal. At. Spectrom.* **2001***, 16*, 774-778.

(21) Pacquette, H. L.; Elwood, S. A.; Ezer, M.; Simeonsson, J. B. *J. Anal. At. Spectrom.* **2001***, 16*, 152-158.

(22) Whanger P *J.Trace Elem.Exp. Med.* **2001***, 13*, 367.

(23) Le, X. C.; Li, X.-F.; Lai, V.; Ma, M.; Yalcin, S.; Feldmann, J. *Spectrochimica Acta Part B: Atomic Spectroscopy* **1998***, 53*, 899-909.

(24) Tsopelas, F. N.; Ochsenkühn-Petropoulou, M. T.; Mergias, I. G.; Tsakanika, L. V. *Anal. Chim. Acta* **2005***, 539*, 327-333.

(25) Health Canada In *Guidelines For Canadian Drinking Water Quality;* Minister of Health: Ottawa, Canada, 1996; , pp 90.

(26) Marchante-Gayón, J. M.; González, J. M.; Fernández, M. L.; Blanco, E.; Sanz-Medel, A. *Fresenius' Journal of Analytical Chemistry* **1996***, 355*, 615-622.

(27) Cannon, H. L. *U.S.Geological Survey Bulletin* **1964***, No*, 127.

(28) National Research Council . Subcommittee on the Tenth Edition of the RDAs.; National Institutes of Health; National Research Council . Committee on Dietary Allowances. Recommended dietary allowances., Eds.; In *Recommended dietary allowances;* National Academy Press: Washington, D.C., 1989; , pp 284.

(29) Hintze, K. J.; Lardy, G. P.; Marchello, M. J.; Finley, J. W. *J. Agric. Food Chem.* **2001***, 49*, 1062-1067.

(30) Verlinden, M. *Talanta* **1981***, 28*, 637.

(31) Qiu, P.; Ai, C.; Lin, L.; Wu, J.; Ye, F. *Microchemical Journal* **2007***, 87*, 1-5.

(32) Zheng, J.; Shibata, Y.; Furuta, N. *Talanta* **2003***, 59*, 27-36.

(33) Pedersen, G. A.; Larsen, E. H. *Fresenius J. Anal. Chem.* **1997***, 358*, 591-598.

(34) Gómez-Ariza, J. L.; Caro de la Torre, M.A.; Giráldez, I.; Morales, E. *Anal. Chim. Acta* **2004***, 524*, 305-314.

(35) Moreda-piñeiro, J.; Cervera, M. L.; de la Guardia, Miguel *J. Anal. At. Spectrom.* **1998***, 13*, 289-293.

(36) Vuchkova, L.; Arpadjan, S. *Talanta* **1996***, 43*, 479-486.

(37) Saisho, H.; Fujimura, Y. *Analytical Sciences* **1990***, 6*, 619.

(38) Ding, W. W.; Sturgeon, R. E. *Spectrochimica Acta Part B: Atomic Spectroscopy* **1996***, 51*, 1325-1334.

(39) Siska, R.; Borszeki, J.; Gegus, E. *Canadian Journal of Applied Spectroscopy.* **1995***, 40*, 117.

(40) Apte, S. C.; Howard, A. G. *J. Anal. At. Spectrom.* **1986***, 1*, 221-225.

(41) Tamer, U.; Pekmez, N. O.; Yildiz, A. *Fresenius Environ. Bull.* **2002***, 11*, 1087.

(42) Liang, P.; Yang, L.; Hu, B.; Jiang, Z. *Analytical Sciences* **2003***, 19*, 1167.

(43) Berthon, G. *Coord. Chem. Rev.* **1996***, 149*, 241-280.

(44) Edwardson J. A. *Jounal of Inorganic Biochemistry* **1991***, 43*, 485.

(45) Cornelis, R.; Heinzow, B.; Herber, R. F. M.; Christensen, J. M.; Poulsen, O. M.; Sabbioni, E.; Templeton, D. M.; Thomassen, Y.; Vahter, M.; Vesterberg, O. *Pure Appl. Chem.* **1995**, 1575-1608.

(46) Pacheco, P. H.; Gil, R. A.; Smichowski, P.; Polla, G.; Martinez, L. D. *Microchemical Journal* **2008***, 89*, 1-6.

(47) Polizzi, S.; Pira, E.; Ferrara, M.; Bugiani, M.; Papaleo, A.; Albera, R.; Palmi, S. *Neurotoxicology* **2002***, 23*, 761-774.

(48) Abu Bakar Tawali, G. Schwedt *Analytical and Bioanalytical Chemistry* **1997***, 357*, 50-55.

(59) Paleologos, E. K.; Giokas, D. L.; Tzouwara-Karayanni, S. M.; Karayannis, M. I. *Anal. Chim. Acta* **2002***, 458*, 241-248.

(50) Kiran Kumar, T. N.; Revanasiddappa, H. D. *Analytical and Bioanalytical Chemistry* **2003***, 376*, 1126-1130.

(51) Burguera, M.; Burguera, J. L.; Rivas, D.; Rondón, C.; Carrero, P.; Alarcón, O. M.; Peña, Yaneira Petit de; Brunetto, M. R.; Gallignani, M.; Márquez, O. P.; Márquez, J. *Talanta* **2005***, 68*, 219-225.

(52) Guerin, T.; Astruc, A.; Astruc, M. *Talanta* **1999***, 50*, 1-24.

(53) Yuan, C.; Jiang, G.; He, B. *J. Anal. At. Spectrom.* **2005***, 20*, 103-110.

(54) Taniguchi, T.; Tao, H.; Tominaga, M.; Miyazaki, A. *J. Anal. At. Spectrom.* **1999***, 14*, 651-655.

(55) Samanta, G.; Chowdhury, U. K.; Mandal, B. K.; Chakraborti, D.; Sekaran, N. C.; Tokunaga, H.; Ando, M. *Microchemical Journal* **2000***, 65*, 113-127.

(56) Wei, X.; Brockhoff-Schwegel, C. A.; Creed, J. T. *J. Anal. At. Spectrom.* **2001***, 16*, 12-19.

(57) Yamini, Y.; Faraji, M.; Shariati, S.; Hassani, R.; Ghambarian, M. *Anal. Chim. Acta* **2008***, 612*, 144-151.

(58) Sayago, A.; Beltrán, R.; Gómez-Ariz, J. L. *J. Anal. At. Spectrom.* **2000***, 15*, 423-428.

(59) Tao, G.; Hansen, E. H. *Analyst* **1994***, 119*, 333-337.

(60) Deng, B.; Feng, J.; Meng, J. *Anal. Chim. Acta* **2007***, 583*, 92-97.

(61) Cutter, G. A. *Anal. Chim. Acta* **1983***, 149*, 391.

(62) Apte, S. C.; Howard, A. G. *J. Anal. At. Spectrom.* **1986***, 1*, 379-382.

(63) El-Hadri, F.; Morales-Rubio, A.; de la Guardia, Miguel *Talanta* **2000***, 52*, 653-662.

(64) Yang, K. X.; Swami, K.; Husain, L. *Spectrochimica Acta Part B: Atomic Spectroscopy* **2002***, 57*, 73-84.

(65) United States Environmental Protection Agency USEPA, Water Related fate of the 129 Priority Pollutants, vol. 1, Washington, DC, 1979 (EP-440/4-79-029A).

(66) *Selenium.* Geneva, World Health Organization, 1987 (Environmental Health Criteria, No. 58).

(67) Zheng, Y.; Lu, J.; Jin, Z.; Cheng, X.; Xu, L. *Fenxi Huaxue* **1989**, *17,* 909.

(68) Cheng, E. A. P.; Fraser, R. D.; Eden, J. G. *Applied Spectroscopy* **1991**, *45,* 949.

(69) Tang, X.; Xu, Z.; Wang, J. *Spectrochimica Acta Part B*, **2005**, *60,* 1580-1585.

(70) Zhang, Y.; Adeloju, S. B. *Talanta*, **2008**, *76,* 724-730.